Scuola di Dottorato Leonardo da Vinci – a.a. 2007/08

LASER: CARATTERISTICHE, PRINCIPI FISICI, APPLICAZIONI

Versione 1 – Luglio 08 – http://www.df.unipi.it/~fuso/dida

Parte 7
Laser a diodo:
realizzazioni convenzionali e non
ed alcune applicazioni

SOMMARIO

- Aspetti di mercato ed innovazione:
  - applicazioni di data storage
  - (possibili) prospettive future

- Laser a giunzione:
  - un po' di storia, omo- ed eterogiunzioni
  - eterostrutture, MQWs e cenni agli eccitoni
  - laser gain ed index guided, DFB, DBR, VCSEL

- Laser a cascata quantica:
  - costruzione
  - principi di funzionamento

Obiettivo : discutere perché e come la microelettronica ha provocato una rivoluzione nella diffusione e nell'impiego dei laser

LASER MARKET ISSUES

Costo approssimativo di dispositivi laser commerciali (ordine di grandezza):
- Laser Ar^+ per applicazioni metrologiche o pompa: decine kE
- Laser CO_2 per applicazioni industriali (saldatura, taglio, etc.): centinaio kE
- Laser eccimeri per marcatura, litografia e trattamento materiali: centinaia kE
- Laser Nd:YAG per applicazioni industriali: centinaio kE
- Laser Ti:Sa al femtosecondo (comprese pompe): centinaia di kE

- Laser a diodo: da pochi Euro a centinaia di Euro (esclusi sistemi alta intensità)!!!

Il laser a diodo, introdotto commercialmente su larga scala a partire da anni '80, ha rivoluzionato il modo di concepire, impiegare, vendere laser!!

La tecnologia rilevante per la fabbricazione è la tecnologia dello stato solido, compreso VLSI (quando possibile)

Applicazioni principali: data storage e TLC, ma esistono anche impieghi di laboratorio e trattamento materiali, medicina, etc.

NOTE STORICHE

The first semiconductor lasers were realized in 1962 almost simultaneously by research groups from General Electric (GE) Laboratories, IBM Research Division, and Massachusetts Institute of Technology (MIT) Lincoln Laboratories. These early devices operated only at cryogenic temperatures or under pulsed conditions. They were homojunction lasers, which means that the same material (GaAs) was used in the active region as well as for the p- and n-doped side of the laser diode junction. In 1963, Herbert Kroemer from the University of Colorado came up with the idea of heterostructure lasers, where a thin active layer is sandwiched between two slabs of different material having a higher band-gap energy to confine the carriers, but it lasted until 1970 before this idea was realized in the AlGaAs/GaAs material system, leading to the first semiconductor lasers that operated continuously at room temperature. In the following two decades, there was a dramatic development in the device properties and an extension of the emission-wavelength range that was mainly driven by the development of fiber communication systems.

Zhores I. Alferov

The Nobel Prize in Physics 2000

Nobel Lecture

Double Heterostructure Concept and its Applications in Physics, Electronics and Technology

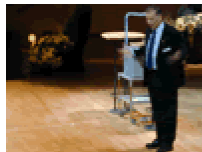

Zhores I. Alferov held his Nobel Lecture December 8, 2000, at Aula Magna, Stockholm University. He was presented by Professor Stig Hagström.

I laser a diodo si basano su concetti e dimostrazioni coevi al laser stesso

ma

evoluzione tecnologica (e.g., MBE) necessaria per maturazione tecnica

(nota: l'evoluzione tecnologica, come al solito, è motivata da applicazioni commercialmente significative!)

FUTURO ORGANICO???

Photonic Frontiers: Organic Semiconductor Lasers - The pump is the challenge

Light-emitting organic semiconductors fall into two broad categories: small molecules and conjugated polymers. Both types are used in OLED fabrication, but laser developers have focused on conjugated polymers, which can be deposited from solution or printed by ink-jet-like devices.

Organic semiconductors have important attractions that extend beyond the ability to fabricate them in inexpensive arrays for OLED displays. In polymers, the semiconducting properties arise from overlap in electron orbits along carbon chains where single and double bonds alternate. Both emission and absorption bands are inherently wide, and wavelength ranges can be chosen by selecting the compounds that make up the polymer. Like laser dyes, both emission bands and absorption bands are broad, allowing both wavelength tuning and short-pulse generation. The absorption bands are strong and widely separated from fluorescence bands, as required for high gain.

Although electrical excitation seems easy for organic LEDs, several issues combine to make it a particularly tough problem for organic semiconductor lasers. One is lower electron mobility than in inorganic semiconductors, which limits current flow in organic materials. Although OLEDs can be driven with a current density of just 0.01 A/cm^2, organic semiconductors can't withstand the current densities of 1000 A/cm^2 needed to drive an inorganic diode laser. To make matters worse, lasers are far more vulnerable to cavity losses than LEDs, and organic diodes suffer losses from electrical contacts and the depletion of excitons by junction current. "The more charge you throw into the cavity, the more excitons get annihilated, so your quantum efficiency gets worse as you pump it harder," says Stephen Forrest of the University of Michigan (Ann Arbor, MI).

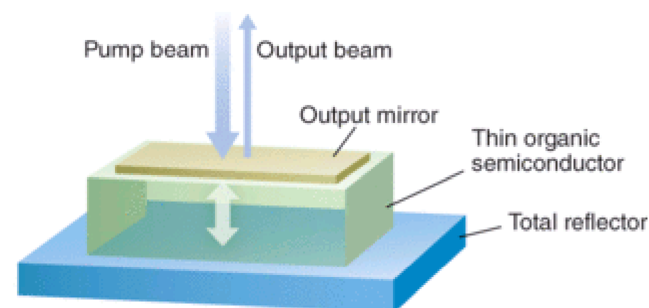

FIGURE 1. Optical pumping of a polymer thin film sandwiched in a Fabry-Perot cavity shows that gain can be high, but power is low because the cavity is very thin.

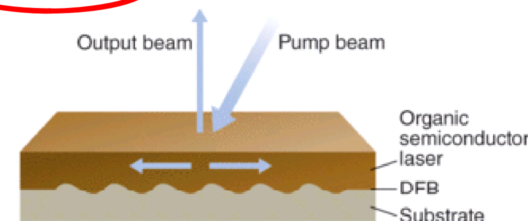

FIGURE 3. A distributed-feedback grating on the substrate scatters light both vertically, to produce the output beam, and horizontally, so the beam can be amplified in the plane of the organic semiconductor layer.

Some key technical issues remain to be overcome, such as improving operating lifetimes of the organic laser materials. But the big question about organic semiconductor lasers is which way the field will go—toward perfecting optically pumped versions or toward a new approach to electrical pumping.

Samuel says that optically pumping with an LED is a key advance toward practical devices. "If you have a low-cost package that gives you a versatile laser that has wires hanging off that you connect to a battery, no one will really care that the charges are injected into the nitride and the light comes from the polymer," he explains. The average user doesn't care if a green-laser pointer is diode-pumped doubled neodymium or direct-diode laser emission, and optical pumping is much easier to achieve. "I'm hopeful that in five years time, rather than wondering when they finally will get injection lasers, I hope they forget why they wanted injection lasers," he says.

Mezzi attivi organici molto promettenti (sintonizzabilità, costi, biocompatibilità, etc.), ma ancora problemi per laser a pompaggio elettronico

UN CENNO SU APPLICAZIONE PRINCIPALE

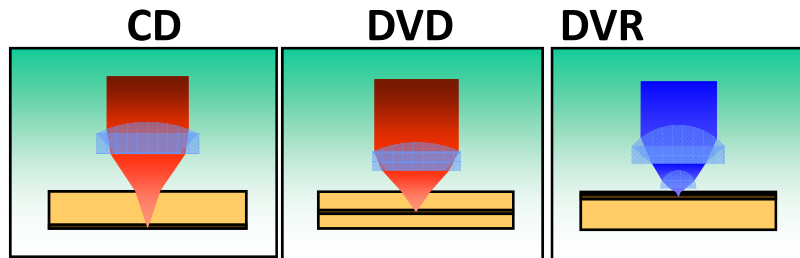

	CD	DVD	DVR
λ (nm)	780	650	400
NA	0.45	0.6	0.85
Capacity (GB)	0.65	4.7	22

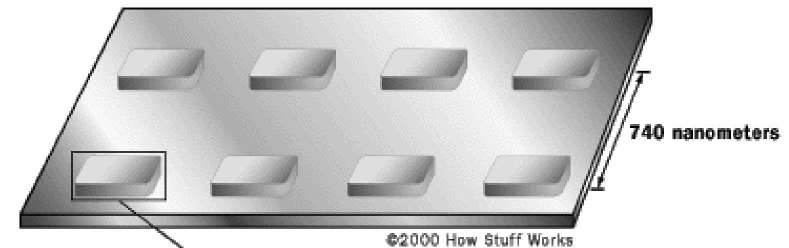

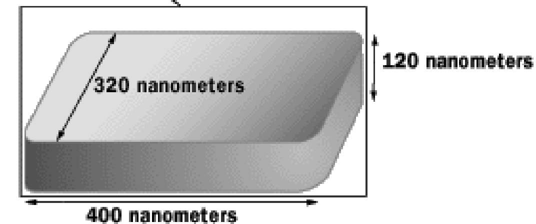

DVD

Parameter	CD	DVD	4th Generation
λ (nm)	780	650	400
NA	0.45	0.60	0.85-1.5
Track pitch (µm)	1.6	0.74	0.3-0.15
Velocity (m s^{-1})	1.2	4.0	3-25
Substrate thickness (mm)	1.2	0.6	1.2-2
Spot size λ/2NA (µm)	0.9	0.55	0.25-0.13
Capacity (GB)	0.65	4.7	100

n.b.: situazione al 2004!

Laser spot minimum size is affected by diffraction ⇩

Optics with larger NA and lasers with shorter wavelength must be used to increase the storage density

$$\text{Abbe limit } (d) = \lambda / 2 \times NA_{obj}$$

Where, d = lateral resolution,
λ = wavelength,
NA_{obj} = numerical aperture of objective.

Luce coerente spazialmente (laser!) necessaria

ULTERIORI SVILUPPI???

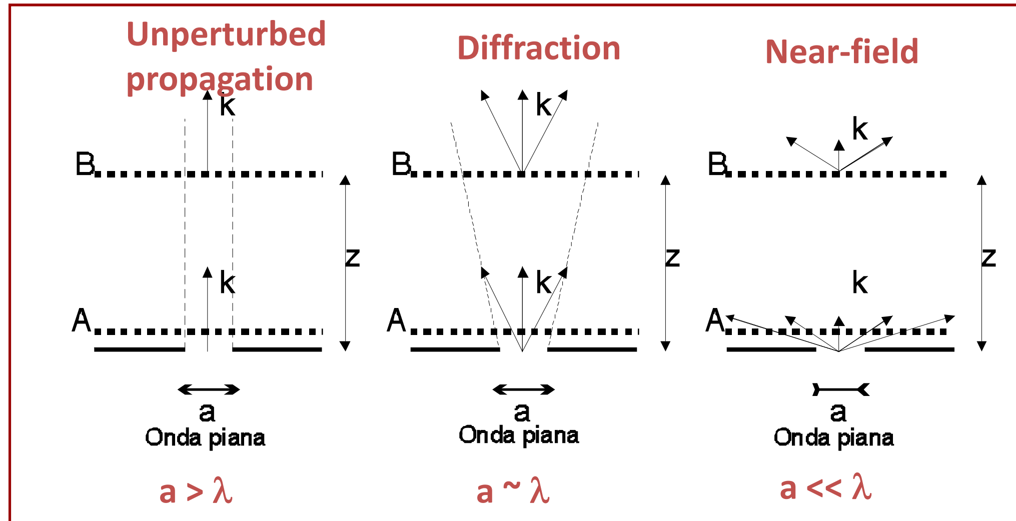

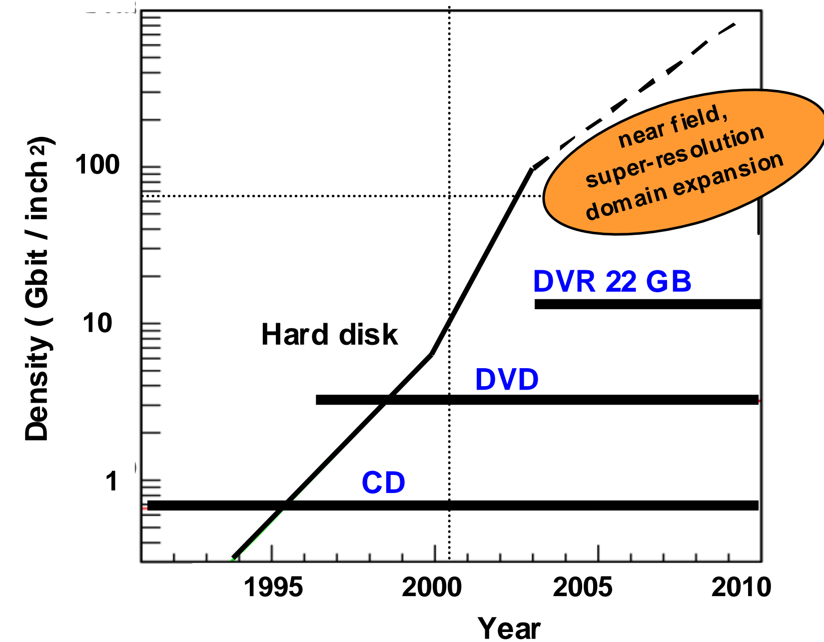

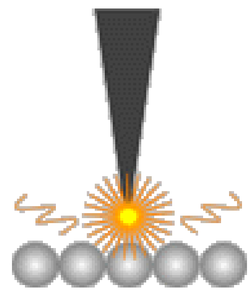

Campo prossimo

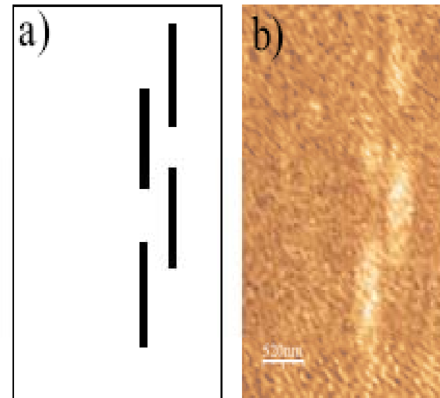

Figure 4.4: a) Representation of the birefringence pattern realized on the free surface of a 30/70 *PMA/PMA4* copolymer film. b) SNOM image of the pattern really realized. In order to read the written information we have used the high-contrast mechanism resulting from polarization modulation that we have implemented in our SNOM setup.

Technological limitations may be (partially) solved, but only alternative approaches hold the possibility to overcome any limit

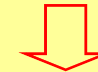

Optical near field??
(we will see more on the tech.)

Luce brillante (laser!) necessaria

MERCATO I

Table 1. Worldwide commercial diode-laser sales 2004–2005 (units)

DIODE UNITS		Materials processing	Medical	Instrumentation	Basic research	Telecommunications	Optical storage	Entertainment	Image recording	Inspection, measurement, and control	Barcode scanning	Sensing	Other	Solid-state laser pumping	TOTALS
<700 nm	2004	50	800	200	0	0	274,500,000	43,000,000	15,000	13,630,000	5,700,000	0	0	0	336,846,050
	2005	100	1,000	300	0	0	341,700,000	43,000,000	17,250	13,660,000	6,300,000	0	0	0	404,678,750
750–980 nm <100 mW	2004	0	0	0	0	0	369,000,000	0	8,600,000	140,000	0	2,300,000	10,210,000	0	390,250,000
	2005	0	0	0	0	0	329,000,000	0	9,100,000	160,000	0	3,700,000	12,050,000	0	354,010,000
750–980 nm 100 mW–10 W	2004	1,250	147,000	600	0	55,000	0	0	93,125	0	0	0	1,000	107,000	404,975
	2005	1,475	162,000	900	0	65,000	0	0	82,500	0	0	0	1,2754	129,000	442,150
750–980 nm >10 W	2004	755	58,500	0	1,000	0	0	0	4,467	0	0	10,000	31,000	19,000	124,722
	2005	855	76,000	0	1,000	0	0	0	5,100	0	0	10,000	31,100	21,133	145,388
908–1550 nm	2004	0	500	0	0	3,622,500	0	0	0	0	0	0	1,536,500	0	5,159,500
	2005	0	500	0	0	4,827,500	0	0	0	0	0	0	1,812,500	0	6,639,500
>1550 nm	2004	0	0	0	0	0	0	0	0	0	0	0	0	0	0
	2005	0	0	0	0	0	0	0	0	0	0	0	0	0	0
Stacks	2004	500	3,250	0	50	0	0	0	0	0	0	0	200	8,250	12,250
	2005	672	3,000	0	50	0	0	0	0	0	0	0	300	9,000	13,022
TOTAL UNITS	2004	2,555	210,050	800	1,050	3,677,500	643,500,000	43,000,000	8,712,592	13,770,000	5,700,000	2,310,000	11,778,700	134,250	732,797,497
	2005	3,102	242,600	1,200	1,050	4,892,500	670,700,000	43,000,000	9,204,850	13,820,000	6,300,000	3,710,000	13,895,175	159,333	765,929,810

Numeri giganteschi di laser a diodo richiesti dal mercato per data storage (e TLC)

MERCATO II

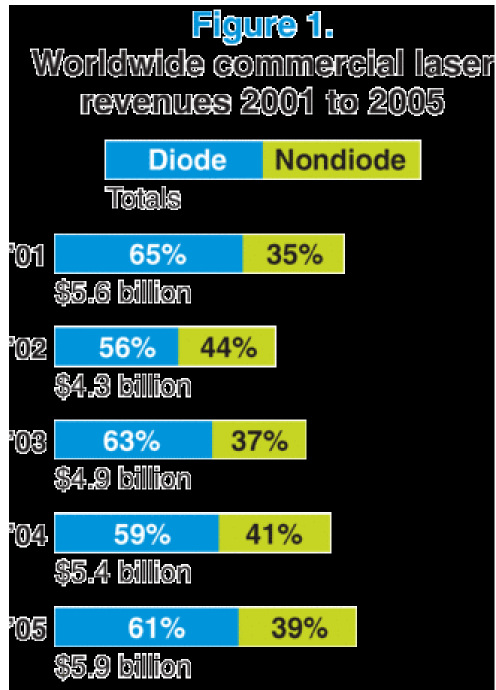

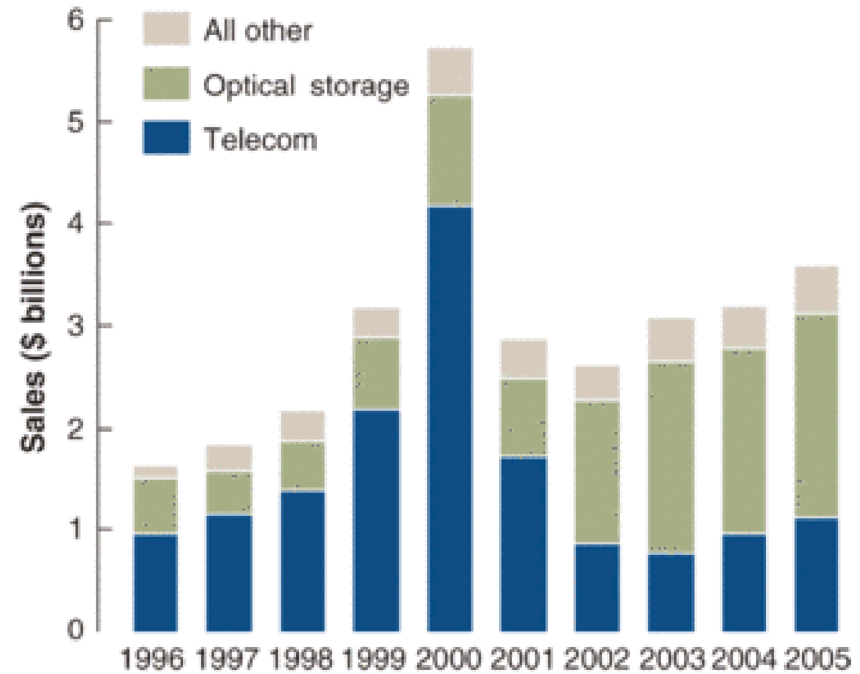

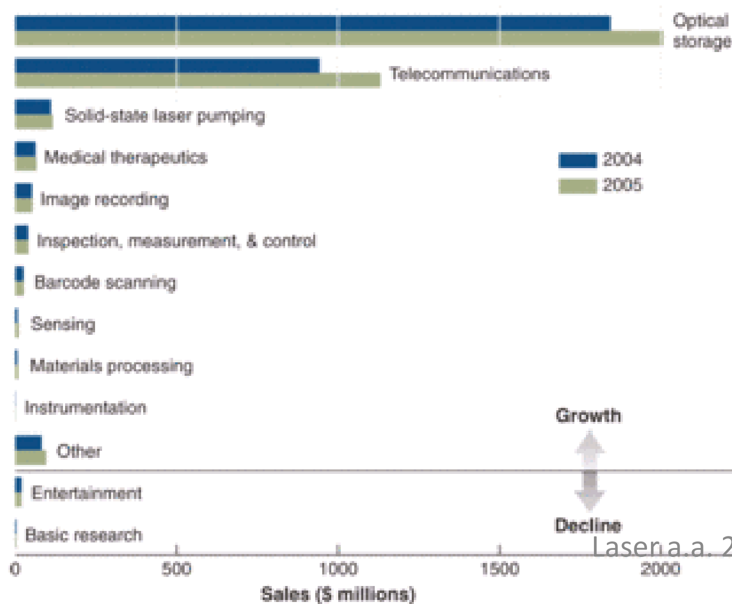

Tendenza alla crescita rallentata (crisi o saturazione?)

SEMICONDUTTORI ED EMISSIONE

Broad diffusion of lasers driven by the availability of solid-state active media, but (bulk) semiconductors, e.g., Si, are not suited because of energy gap (in the IR) and indirect transitions

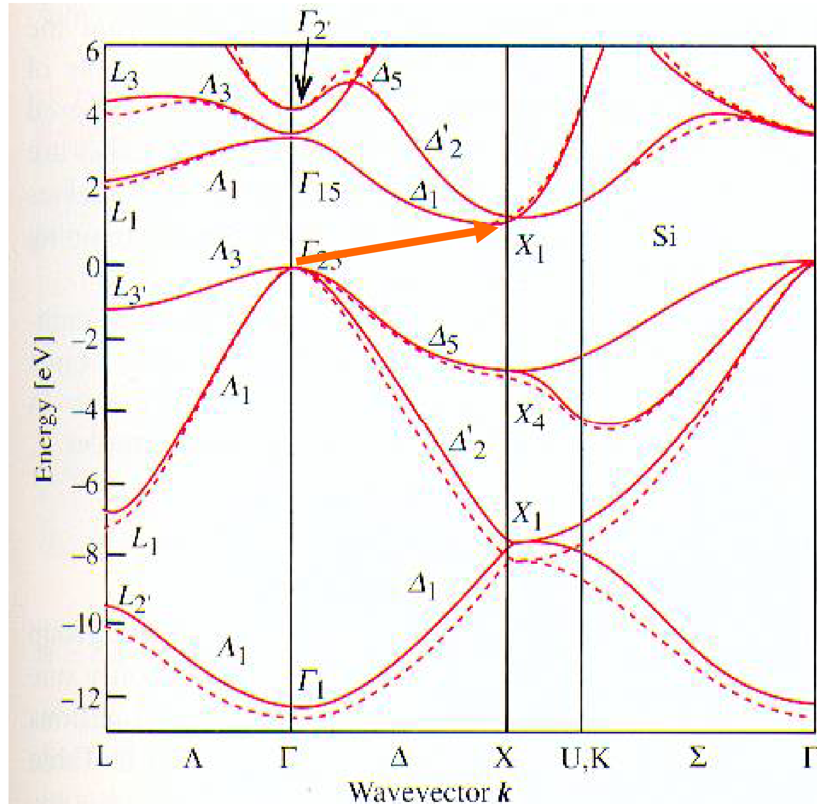

Fig. 2.10. Electronic band structure of Si calculated by the pseudopotential technique. The *solid* and the *doted lines* represent calculations with a **nonlocal** and a **local pseudopotential**, respectively. [Ref. 2.6, p. 81]

Fundamentals of Semicond. Springer (1996)

Band structure of Si

The top of valence band and the bottom of the conduction band are displaced each other

⇩

Momentum conservation implies phonons to be involved in the absorption process

⇩

Transition probability is small (10^{-5}-10^{-6} s^{-1}) (and wavelength is in the IR, above 1 μm)

Bulk semiconductive materials with indirect gap can be hardly used in electroluminescent devices

LEGHE III-V

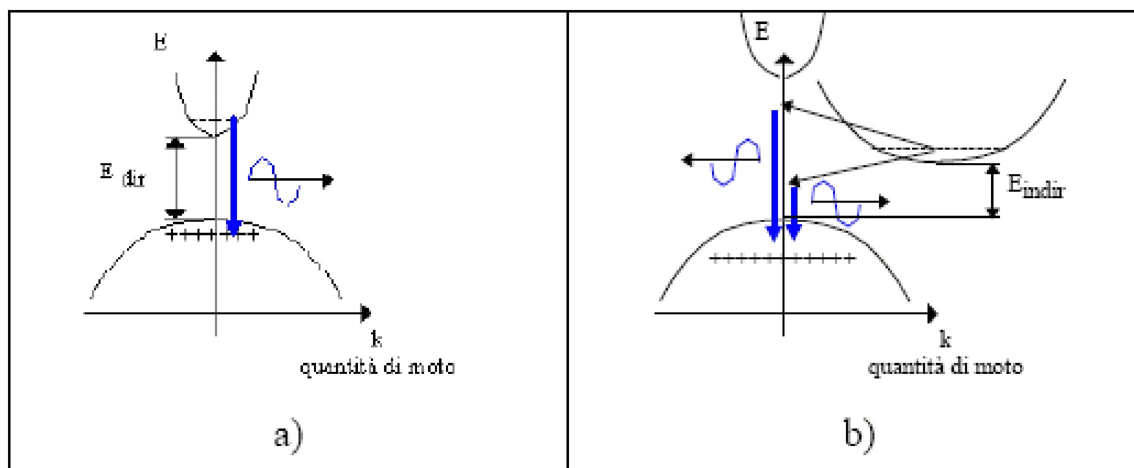

Figura 3.5.13. Struttura di banda di un semiconduttore a gap diretta (a) e a gap indiretta (b), e transizione radiante.

Gap diretto offre efficienza quantica interna molto superiore

Materiali	Salto energetico [ev]	Tipo
GaN	3,5	diretto
SiN	2,8÷3,2	indiretto
$Al_x Ga_{1-x} P$	2,26÷2,45	indiretto
Ga AS	1,44	diretto
GaP	2,26	indiretto
AlAs	2,16	indiretto
$In_{1-x} Ga_x P$	1,34÷2,26	dir-indiretto
$In_{1-x} Al_x P$	1,34÷2,45	dir-indiretto
$Al_x Ga_{1-x} As$	1,44÷2,16	dir-indiretto
$Ga As_{1-x} P_x$	1,44÷2,26	dir-indiretto

Come si può vedere dalla Figura 3.5.14, dove x indica la percentuale del materiale a gap indiretta, il semiconduttore si comporta da diretta fino a quando x raggiunge circa il 40%; semiconduttori di questo tipo vengono detti a gap energetica *maggiorata*. Questi materiali consentono di variare la frequenza della radiazione emessa pur mantenendo un'elevata radianza.

Maggiorazione gap dovuta a concentrazione relativa *x*

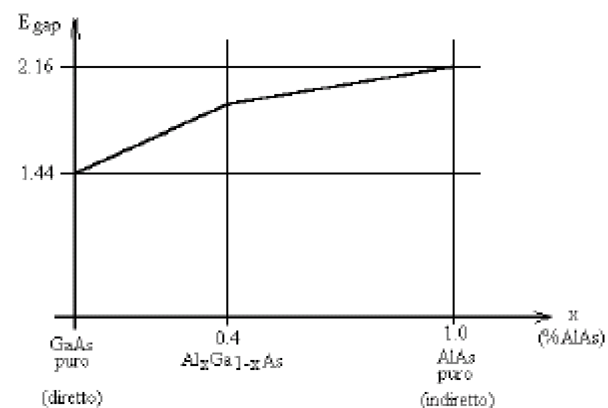

Leghe III-V presentano gap in vasto intervallo di energia e possono avere gap diretto

PRIMI LASER A DIODO

For Hall, who already had extensive experience with GaAs alloy junctions, tunnel diodes, and light-emitting diodes, the project to make a laser diode was an extension of his prior research work. It also coupled well with his optical experience in his earlier youthful hobbyist efforts to build telescopes and to polish lenses and mirrors [3]. Hall's laser project team included Dick Carlson, Gunther Fenner, Jack Kingsley, and Ted Soltys. Whereas other groups thinking about semiconductor lasers had proposed to use a macroscopic "external cavity" into which a GaAs diode was placed, Hall decided to polish parallel faces onto his GaAs diodes so that the Fabry- Perot optical cavity geometry was built into the device. This approach was not universally applied and, in fact, the importance of optical feedback into the diode "active region" was not fully appreciated by many workers. Hall's team operated their first successful GaAs laser diodes under pulsed conditions at 77K on September 16, 1962 [1]. A schematic diagram of Hall's early concept for an injection laser is shown in Figure 1. The first

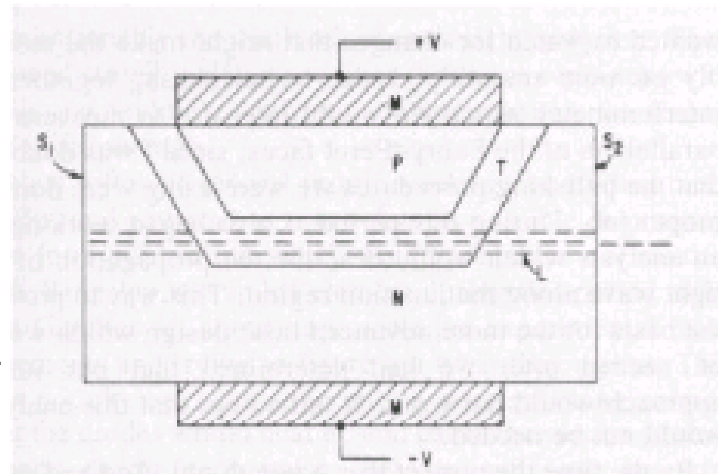

Figure 1: Schematic diagram of initial concept for an injection laser developed at General Electric Research Laboratories by Robert Hall in 1962.

© 1987/2000 IEEE

Omogiunzione in diodo GaAs

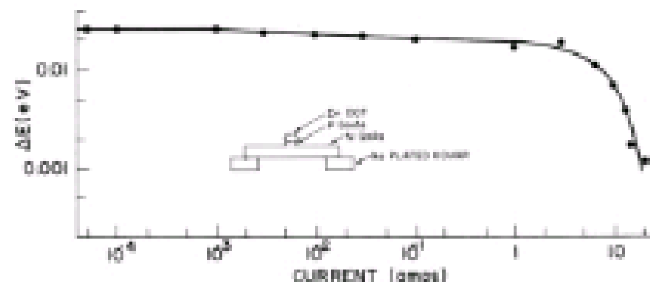

Figure 2: Spectral linewidth vs. current for a GaAs diode made at IBM and operated at 77K. The diode did not have a Fabry-Perot geometry so cavity modes were not observed.

© 1987/2000 IEEE

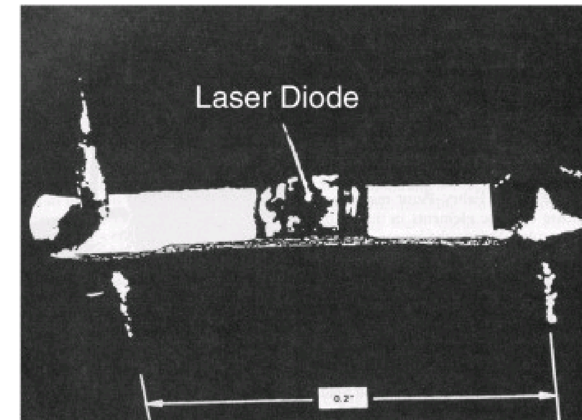

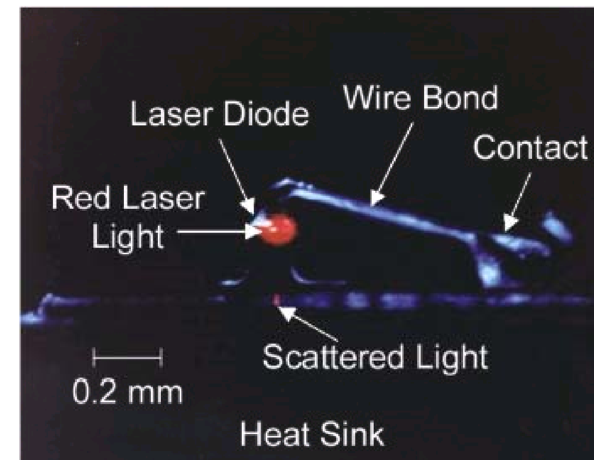

Mezzo attivo : ricomb inazione *e-h* in giunzione
Poco interesse per ottica cavità!!

RIFLESSIONE TRA DIELETTRICI

When light moves from a medium of a given refractive index n_1 into a second medium with refractive index n_2, both reflection and refraction of the light may occur.

In the diagram on the right, an incident light ray **PO** strikes at point **O** the interface between two media of refractive indexes n_1 and n_2. Part of the ray is reflected as ray **OQ** and part refracted as ray **OS**. The angles that the incident, reflected and refracted rays make to the normal of the interface are given as θ_i, θ_r and θ_t, respectively. The relationship between these angles is given by the law of reflection and Snell's law.

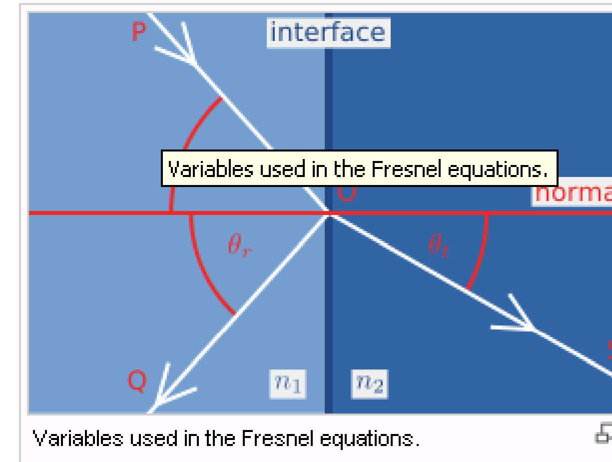

Variables used in the Fresnel equations.

The fraction of the intensity of incident light that is reflected from the interface is given by the *reflection coefficient* R, and the fraction refracted by the *transmission coefficient* T. The Fresnel equations, which are based on the assumption that the two materials are both *non-magnetic*, may be used to calculate R and T in a given situation. The following fields are continuous: tangential E and H, normal B and D.

The calculations of R and T depend on polarisation of the incident ray. If the light is polarised with the electric field of the light perpendicular to the plane of the diagram

$$R_s = \left[\frac{\sin(\theta_t - \theta_i)}{\sin(\theta_t + \theta_i)}\right]^2 = \left[\frac{n_1 \cos(\theta_i) - n_2 \cos(\theta_t)}{n_1 \cos(\theta_i) + n_2 \cos(\theta_t)}\right]^2 = \left[\frac{n_1 \cos(\theta_i) - n_2 \sqrt{1 - \left(\frac{n_1}{n_2} \sin\theta_i\right)^2}}{n_1 \cos(\theta_i) + n_2 \sqrt{1 - \left(\frac{n_1}{n_2} \sin\theta_i\right)^2}}\right]^2$$

where θ_t can be derived from θ_i by Snell's law and is simplified using trigonometric identities.

If the incident light is polarised in the plane of the diagram (*p*-polarised), the R is given by:

$$R_p = \left[\frac{\tan(\theta_t - \theta_i)}{\tan(\theta_t + \theta_i)}\right]^2 = \left[\frac{n_1 \cos(\theta_t) - n_2 \cos(\theta_i)}{n_1 \cos(\theta_t) + n_2 \cos(\theta_i)}\right]^2 = \left[\frac{n_1 \sqrt{1 - \left(\frac{n_1}{n_2} \sin\theta_i\right)^2} - n_2 \cos(\theta_i)}{n_1 \sqrt{1 - \left(\frac{n_1}{n_2} \sin\theta_i\right)^2} + n_2 \cos(\theta_i)}\right]^2$$

The transmission coefficient in each case is given by $T_s = 1 - R_s$ and $T_p = 1 - R_p$.

If the incident light is unpolarised (containing an equal mix of *s*- and *p*-polarisations), the reflection coefficient is $R = (R_s + R_p)/2$.

When the light is at near-normal incidence to the interface (θ_i

$$R = R_s = R_p = \left(\frac{n_1 - n_2}{n_1 + n_2}\right)^2$$

$$T = T_s = T_p = 1 - R = \frac{4 n_1 n_2}{(n_1 + n_2)^2}$$

GaAs: n~3.7

→ $R_{orthogonal}$~0.33

Nota: n dipende da drogaggio e, nelle leghe (soluzioni solide) anche da concentrazione materiali

LASER A OMOGIUNZIONE

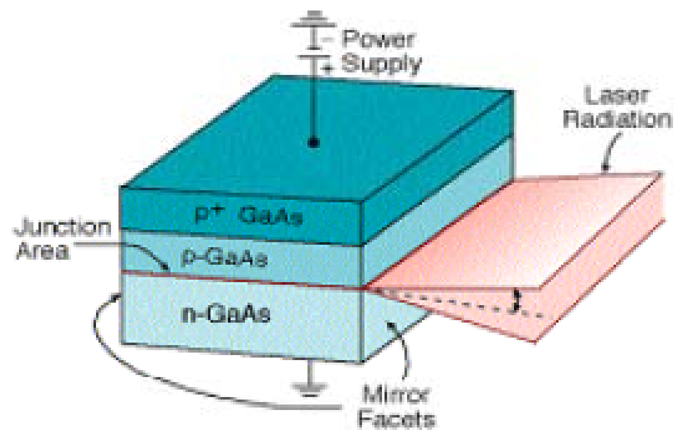

Figura 3.5.15
Schema di un laser a omogiunzione

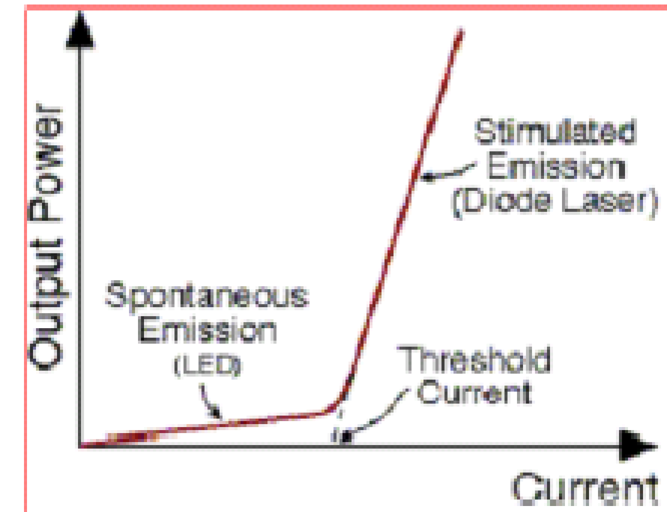

These layers of semiconductor materials are arranged such that at the p-n junction an active region is created, in which photons are created by the recombination process. On the top and bottom layers, a layer of metal allows connecting external voltage to the laser. The voltage is applied to metal contacts above and below the semiconductor layers. The side of the crystalline semiconductor are cut to serve as mirrors at the end of the optical cavity.

The radiation comes out of a rectangular shape of a very thin active layer, and spreads at different angles in 2 directions.

If the condition of population inversion does not exist, the photons will be emitted by spontaneous emission. These photons will be emitted randomly in all directions, that is the basis of operation of a light emitting diode (LED). The condition for population inversion depends on the pumping. By increasing the current injected through the p-n junction, we arrive at threshold current, which fulfills this condition.It is easily seen that the slope of this graph in a stimulated emission (laser) is far greater than the slope at spontaneous emission (LED).

The threshold current for lasing is determined by the intercept of the tangent to the graph at stimulated emission with the current axis (this point is very close to the point of change in the slope). When the current threshold is low, less energy will be wasted in the form of heat, and more energy will be transmitted as laser radiation. Practically, the important parameter is current density (A/cm^2).

Mezzo attivo è nella giunzione

Poco materiale
Scarsa qualità ottica

Cavità realizzata da interfaccia giunzione/aria

Forti perdite, scarso *Q*

LIMITI OMOGIUNZIONE

Problema fondamentale omogiunzione:
fotoni non confinati in direzione trasversa all'asse
→ forti perdite ottiche
→ necessità alte correnti di iniezione
→ scarsa durata

Laser a omogiunzione

The entire laser is made from one substance, usually GaAs. In this simple structure, the emitted photons are not confined in the directions perpendicular to the laser axis. Thus, the laser is not efficient.

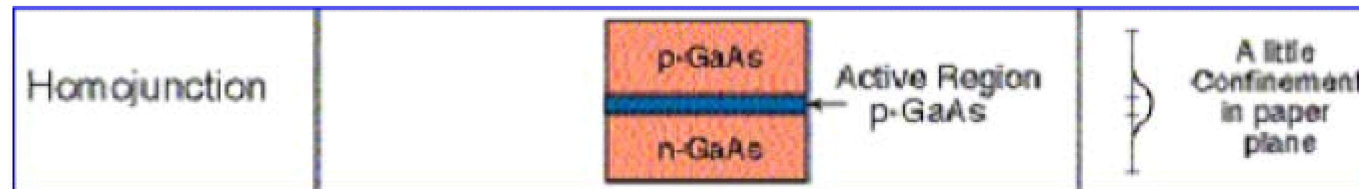

Laser ad eterogiunzione

La causa principale dell'alta corrente di soglia nei normali diodi laser, sopratutto a temperatura ambiente, nasce dalla difficoltà di confinare gli elettroni e le lacune nella regione della giunzione. A causa del coefficiente di diffusione dei portatori iniettati, che cresce con la temperatura, è difficile mantenere nella regione della giunzione una apprezzabile inversione di popolazione, a meno di un continuo ricambio di cariche iniettate dalla corrente. Un geniale rimedio allo sparpagliamento dei portatori è stato ottenuto con il laser ad eterogiunzione nel quale la corrente di soglia è di oltre un ordine di grandezza più bassa di quella del laser ad omogiunzione finora descritto.

MBE ARTEFICE DEL PROGRESSO

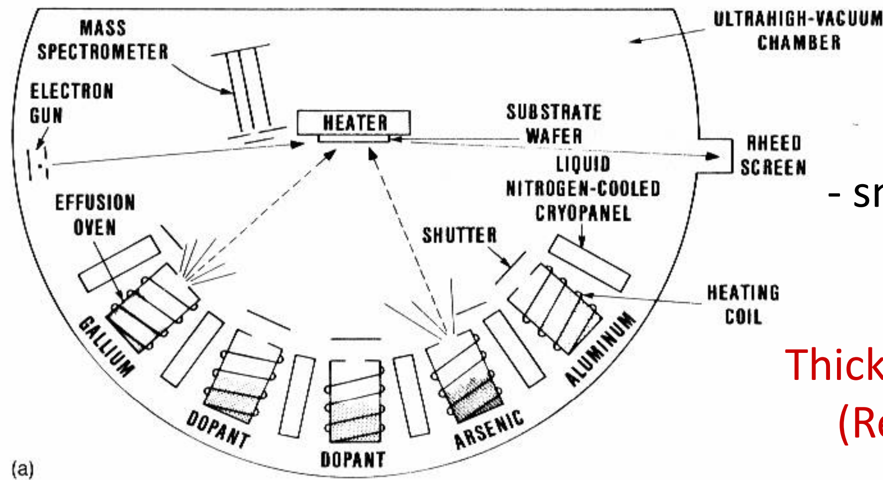

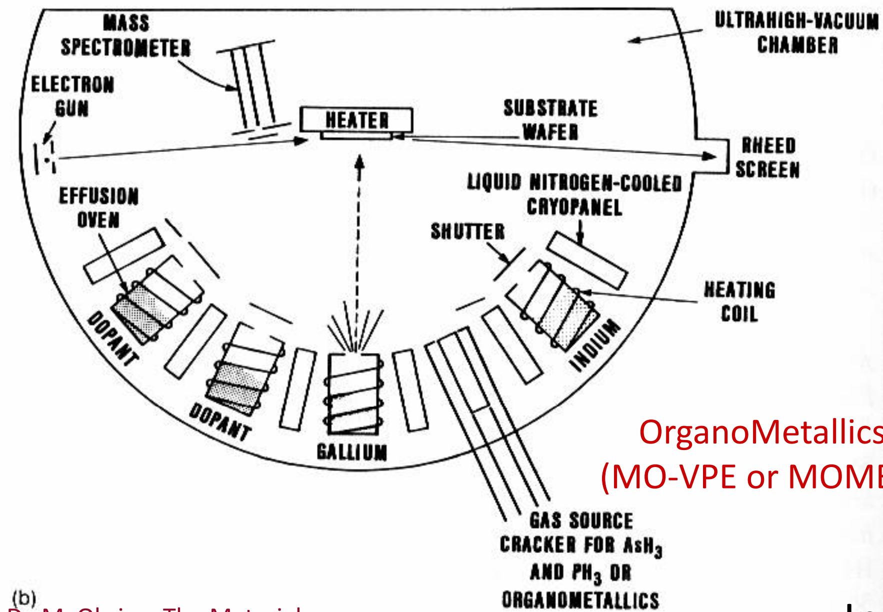

Da M. Ohring, The Materials Science of Thin Films, Academic (1992)

OrganoMetallics (MO-VPE or MOMBE)

Key points for MBE:
- clean process (UHV, $p \leq 10^{-10}$mbar)
- small continuous deposition rate (~ 1 μm/h)
- suitable with semiconductor

⇩

Thickness easily controlled at the monolayer level
(Relatively) low kinetic energy favors epitaxy
Heterostructures easily fabricated

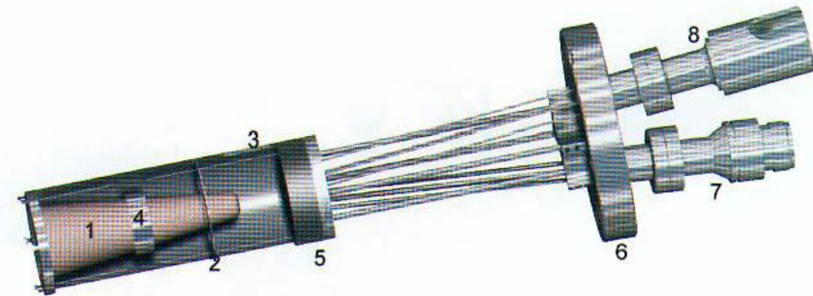

Example of effusive oven (MPI)

Inert materials used (but difficult with oxides!)

CRESCITA PSEUDOMORFA

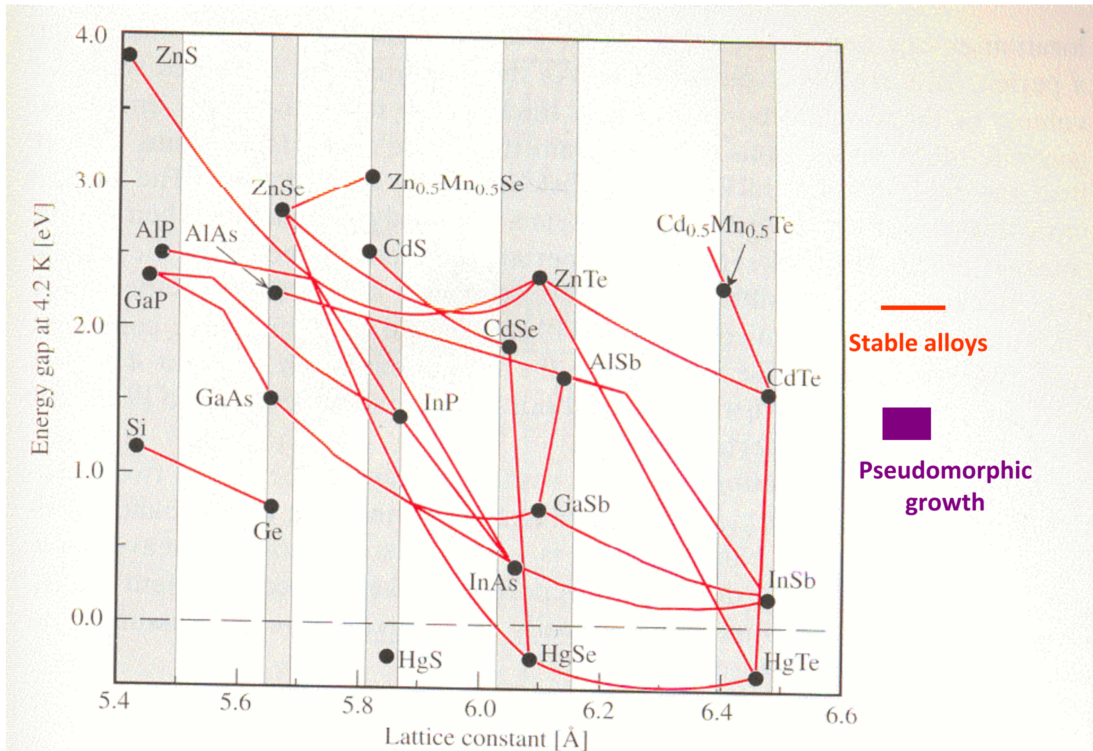

Fig. 9.2. A plot of the low temperature energy bandgaps of a number of semiconductors with the diamond and zinc-blende structure versus their lattice constants. The *shaded regions* highlight several families of semiconductors with similar lattice constants. Semiconductors joined by *solid lines* form stable alloys. [Chen A.B., Sher A.: *Semiconductor Alloys* (Plenum, New York 1995) Plate 1]

Stable alloys

Pseudomorphic growth

A wide choice of semiconductors is available to tune the gap in a broad range (from blue to near-IR)
→ Band engineering through materials

Now, higher gaps achieved with GaN

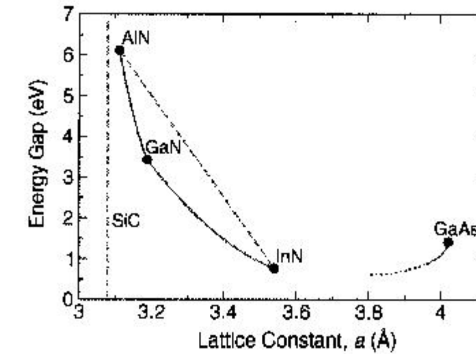

Figure 1. Fundamental bandgap versus basal-plane lattice constant of nitride materials compared with SiC and GaAs. The solid curves represent the ternary mixtures AlN/GaN,[10] GaN/InN,[11] and GaN/GaAs.[12] The dotted curve qualitatively indicates the continuation of the GaNAs gap toward GaN.

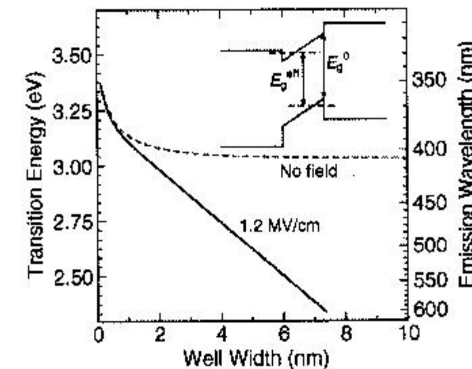

Figure 3. Transition energy of $Ga_{0.9}In_{0.1}N$/GaN quantum wells versus well width, with and without built-in electric field. The inset shows a schematic view of the band scheme, the effective bandgap E_g^{eff}, and the original bandgap E_g^0.

See MRS Bull. 27 (July 2002)

ETEROGIUNZIONI SINGOLE E MULTIPLE

Alternando strati di materiali diversi si ottiene confinamento dei fotoni in direzione trasversale (direzione di crescita)

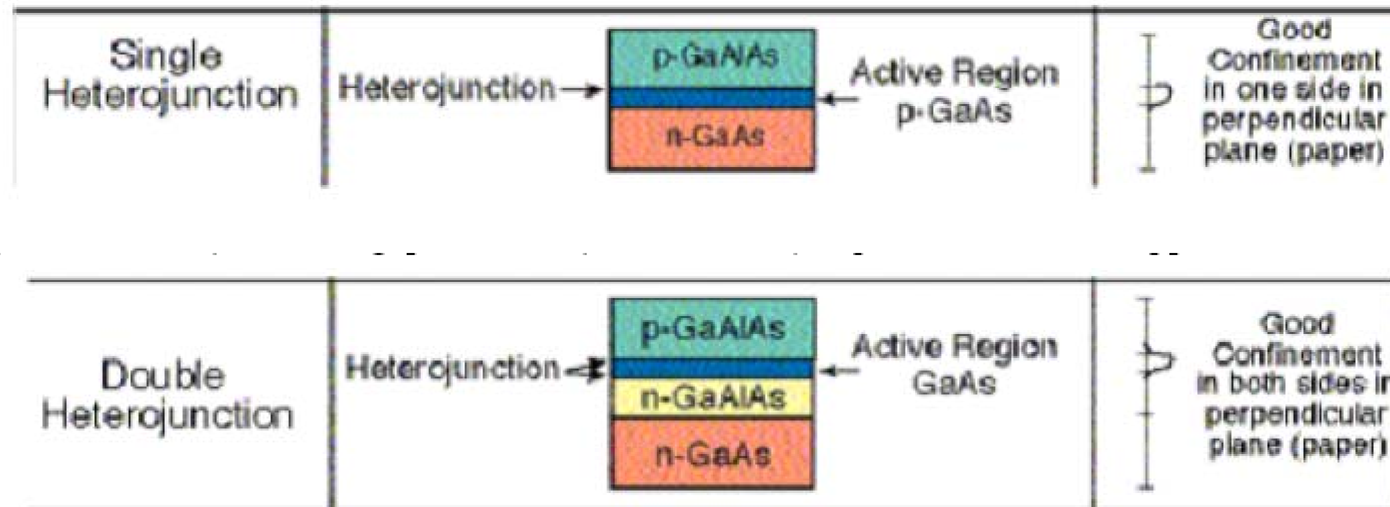

Si può avere confinamento radiazione anche nell'altra direzione trasversa (piano della giunzione) definendo lateralmente concentrazione/drogaggio

(Gain or) index guided lasers

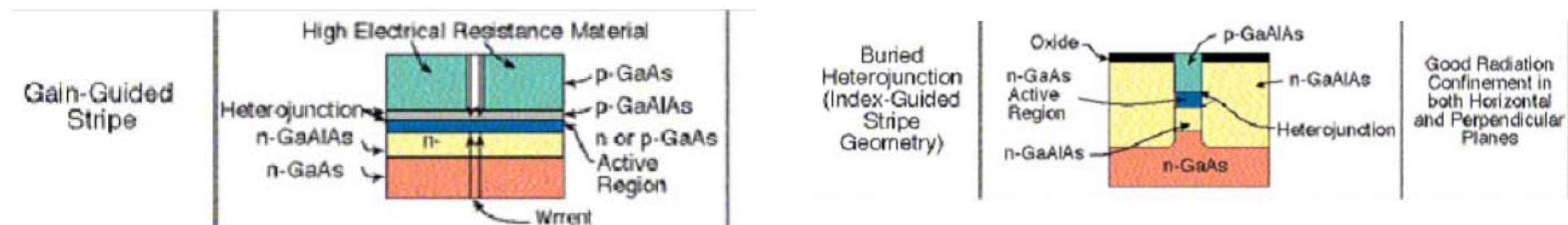

ETEROSTRUTTURE

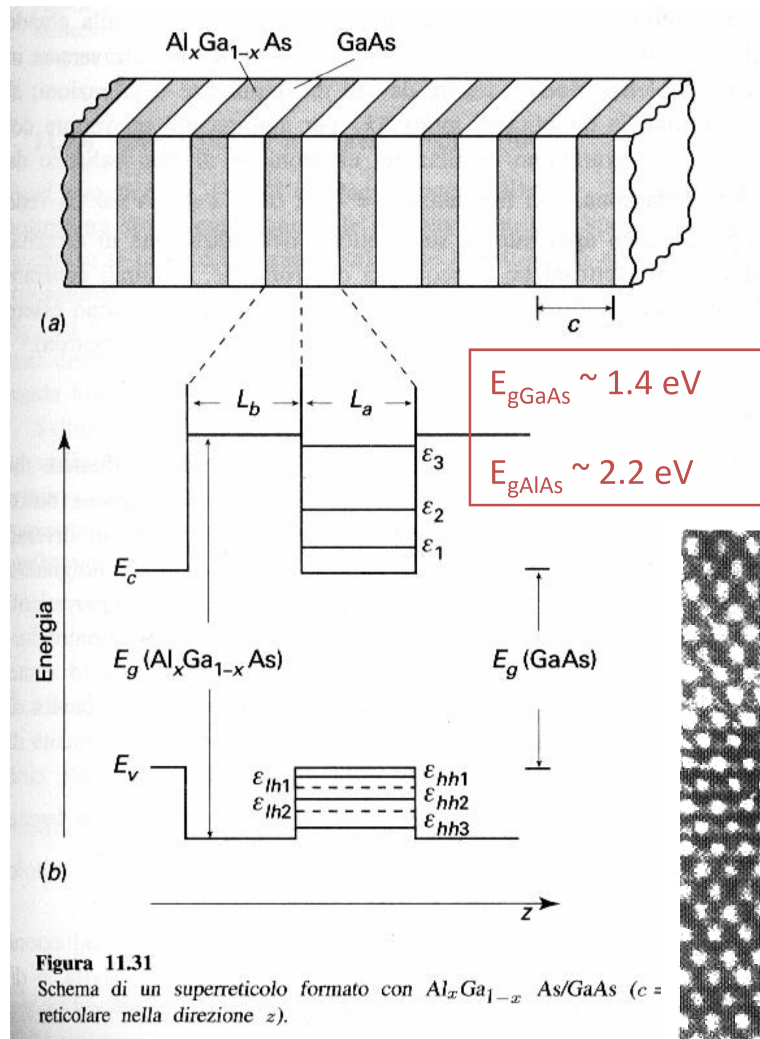

Figura 11.31
Schema di un superreticolo formato con Al_xGa_{1-x} As/GaAs (c = reticolare nella direzione z).

Heterostructures(superlattices): sequence of layers made of semiconductors with different gap energies (*as we have already seen!)*

E_{gGaAs} ~ 1.4 eV

E_{gAlAs} ~ 2.2 eV

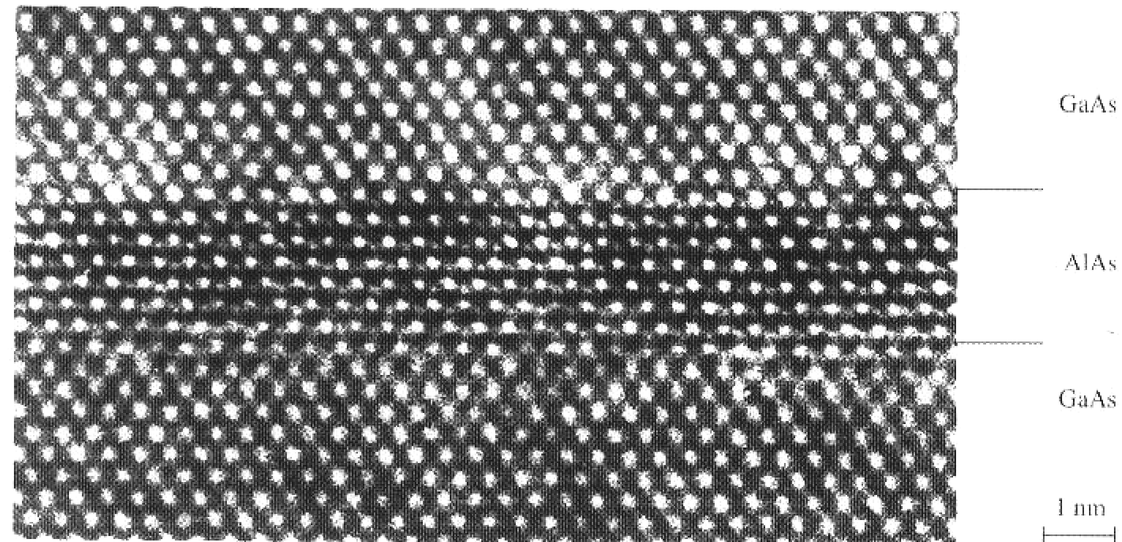

Fig. 9.1. High resolution transmission electron micrograph (TEM) showing a GaAs/AlAs superlattice for a [110] incident beam. (Courtesy of K. Ploog, Paul Drude Institute, Berlin.) In spite of the almost perfect interfaces, try to identify possible Al atoms in Ga sites and vice versa

Da Bassani Grassano, Fisica dello Stato Solido, Boringhieri (2000)

MULTIPLE QUANTUM WELLS (MQWs)

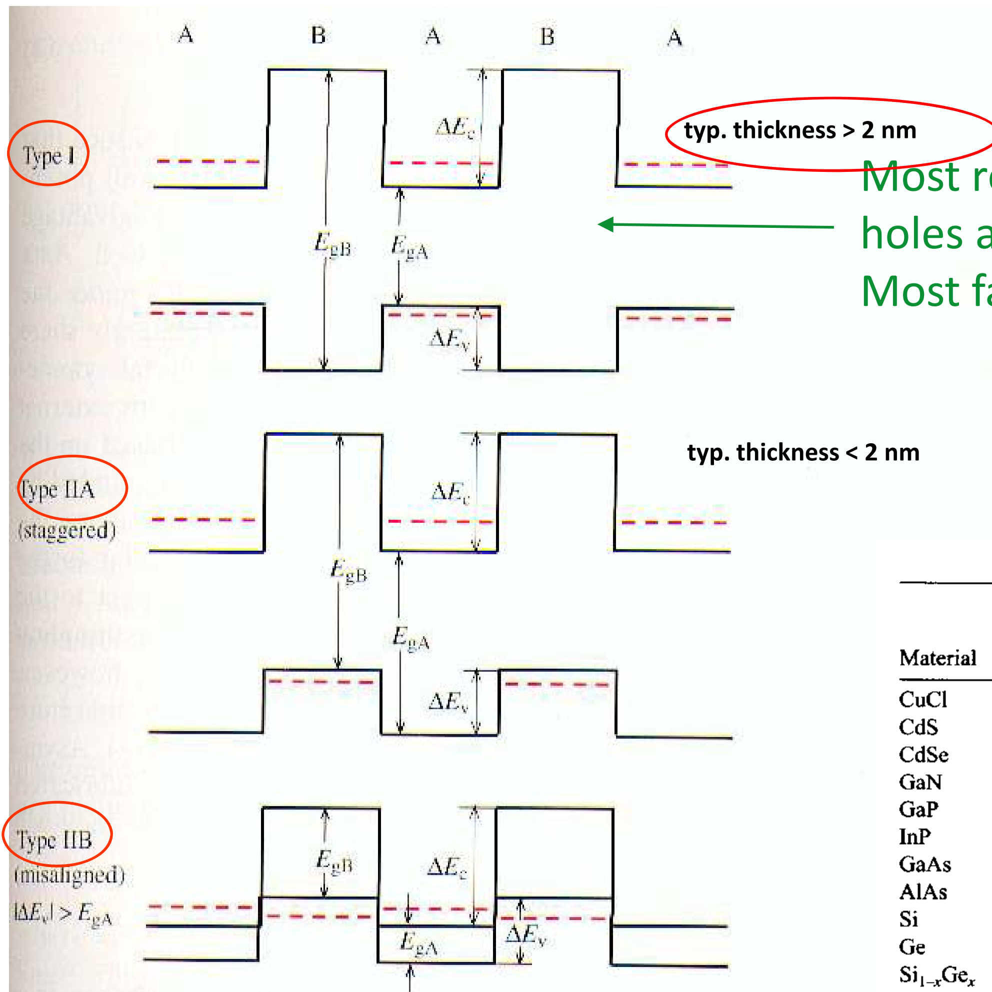

Most relevant configuration: electrons and holes are confined in the same layer

Most favoured for exciton formation

e.g.: A=GaAs (E_{gA} ~ 1.4 eV, lattice 5.653 Å)
B=AlAs (E_{gB} ~ 2.2 eV, lattice 5.62 Å)
or B=$Ga_{1-x}Al_xAs$ (x typ. ≤ 0.3)

Fig. 9.3. Schematic diagrams of three arrangements of the confinement holes in MQWs and superlattices formed by two semiconductors A and E_{gA} and E_{gB}, respectively. In type I samples both the electrons and holes are confined in the same layer A. The energies of the confined particles are represented by *red lines*. In type IIA systems the electrons and holes are confined in different layers. Type IIB samples are a special case of type IIA behavior. They are either small gap semiconductors or semimetals

Table 4.1. Semiconductor Material Parameters

Material	Periodic Table Classification	Bandgap Energy (eV)	Bandgap Wavelength (μm)	Exciton Bohr Radius (nm)	Exciton Binding Energy (meV)
CuCl	I–VII	3.395	0.36	0.7	190
CdS	II–VI	2.583	0.48	2.8	29
CdSe	II–VI	1.89	0.67	4.9	16
GaN	III–V	3.42	0.36	2.8	
GaP	III–V	2.26	0.55	10–6.5	13–20
InP	III–V	1.35	0.92	11.3	5.1
GaAs	III–V	1.42	0.87	12.5	5
AlAs	III–V	2.16	0.57	4.2	17
Si	IV	1.11	1.15	4.3	15
Ge	IV	0.66	1.88	25	3.6
$Si_{1-x}Ge_x$	IV	$1.15–0.874x + 0.376x^2$	$1.08–1.42x + 3.3x^2$	$0.85–0.54x + 0.6x^2$	$14.5–22x + 20x^2$
PbS	IV–VI	0.41	3	18	4.7
AlN	III–V	6.026	0.2	1.96	80

MQW II

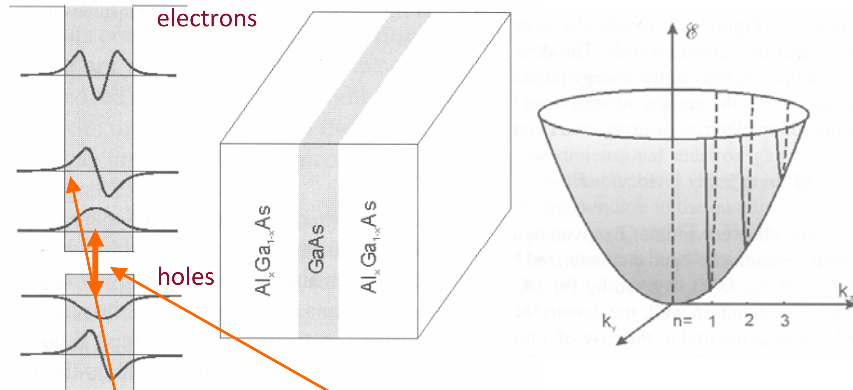

- For energies $E < V$, the energy levels of the electron are quantized for the direction z of the confinement; hence they are given by the model of particle in a one-dimensional box. The electronic energies in the other two dimensions (x and y) are not discrete and are given by the effective mass approximation discussed in Chapter 2. Therefore, for $E < V$, the energy of an electron in the conduction band is given as

$$E_{n,k_x,k_y} = E_C + \frac{n^2h^2}{8m_e^* l^2} + \frac{\hbar^2(k_x^2 + k_y^2)}{2m_e^*} \qquad (4.1)$$

where $n = 1, 2, 3$ are the quantaum numbers. The second term on the right-hand side represents the quantized energy; the third term gives the kinetic energy of the electron in the x–y plane in which it is relatively free to move. The symbols used are as follows: m_e^* is the effective mass of electron, and E_C is the energy corresponding to the bottom of the conduction band.

Equation (4.1) shows that for each quantum number n, the values of wavevector components k_x and k_y form a two-dimensional band structure. However, the wavevector k_z along the confinement direction z takes on only discrete values, $k_z = n\pi/l$. Each of the bands for a specific value of n is called a sub-band. Thus n becomes a sub-band index. Figure 4.2 shows a two-dimensional plot of these sub-bands.

- For $E > V$, the energy levels of the electron are not quantized even along the z direction. Figure 4.1 shows that for the AlGaAs/GaAs quantum well, the quantized levels $n = 1$–3 exist, beyond which the electronic energy level is a continuum. The total number of discrete levels is determined by the width l of the well and the barrier height V.

- The holes behave in analogous way, except their quantized energy is inverted and the effective mass of a hole is different. Figure 4.1 also shows that for the holes, two quantized states with quantum numbers $n = 1$ and 2 exist for this particular quantum well (determined by the composition of AlGaAs and the width of the well). In the case of the GaAs system, two types of holes exist, determined by the curvature (second derivative) of the band structure. The one with a smaller effective mass is called a *light hole* (lh), and the other with a heavier effective mass is called a *heavy hole* (hh). Thus the $n = 1$ and $n = 2$ quantum states actually are each split in two, one corresponding to lh and the other to hh.
- Because of the finite value of the potential barrier ($V \neq \infty$), the wavefunctions, as shown for levels $n = 1$, 2, and 3 in the case of electrons and levels $n = 1$ and 2 in the case of holes, do not go to zero at the boundaries. They extend into the region of the wider bandgap semiconductor, decaying exponentially into this region. This electron leakage behavior has already been discussed in Section 2.1.3 of Chapter 2.
- The lowest-energy band-to-band optical transition (called the interband transition) is no longer at E_g, the energy gap of the smaller bandgap semiconductor, GaAs in this case. It is at a higher energy corresponding to the difference between the lowest energy state ($n = 1$) of the electrons in the conduction band and the corresponding state of the holes in the valence band. The effective bandgap for a quantum well is defined as

$$E_g^{\text{eff}} = (E_C - E_V) + \frac{h^2}{8l^2}\left(\frac{1}{m_e^*} + \frac{1}{m_h^*}\right) \qquad (4.2)$$

In addition, there is an excitonic transition below the band-to-band transition. These transitions are modifications of the corresponding transitions found for a bulk semiconductor. In addition to the interband transitions, new transitions between the different sub-bands (corresponding to different n values) within the conduction band can occur. These new transitions, called intraband or inter-sub-band transitions, find important technologic applications such as in quantum cascade lasers. The optical transitions in quantum-confined structures are further discussed in the next section.

Da P.N. Prasad, *Nanophotonics*, Wiley (2004)

MQW III

- Another major modification, introduced by quantum confinement, is in the density of states. The density of states $D(E)$, defined by the number of energy states between energy E and $E + dE$, is determined by the derivative $dn(E)/dE$. For a bulk semiconductor, the density of states $D(E)$ is given by $E^{1/2}$. For electrons in a bulk semiconductor, $D(E)$ is zero at the bottom of the conduction band and increases as the energy of the electron in the conduction band increases. A similar behavior is exhibited by the hole, for which the energy dispersion (valence band) is inverted. Hence, as the energy is moved below the valence band maximum, the hole density of states increases as $E^{1/2}$. This behavior is shown in Figure 4.3, which also compares the density of states for electrons (holes) in a quantum well. The density of states is a step function because of the discreteness of the energy levels along the z direction (confinement direction). Thus the density of states per unit volume for each sub-band, for example for an electron, is given as a rise in steps of

$$D(E) = m_e^*/\pi^2 \qquad \text{for } E > E_1 \qquad (4.3)$$

The steps in $D(E)$ occur at each allowed value of E_n given by Equation (4.1), for k_x and $k_y = 0$, then stay constant for each sub-band characterized by a specific n (or k_z). For the first sub-band with $E_n = E_1$, $D(E)$ is given by Eq. (4.3). This step-like behavior of $D(E)$ implies that for a quantum well, the density of states in the vicinity of the bandgap is relatively large compared to the case of a bulk semiconductor for which $D(E)$ vanishes. As is discussed below, a major manifestation of this modification of the density of states is in the strength of optical transition. A major factor in the expression for the strength of optical transition (often defined as the oscillator strength) is the density of states. Hence, the oscillator strength in the vicinity of the bandgap is considerably enhanced for a quantum well compared to a bulk semiconductor. This enhanced oscillator strength is particularly important in obtaining laser action in quantum wells, as discussed in Section 4.4.

DOS

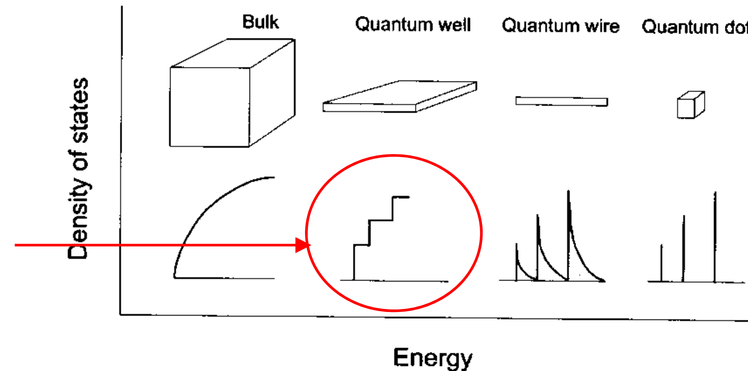

Figure 4.3. Density of states for electrons in bulk conduction band together with those in various confined geometries.

Optical transitions in quantum confined systems

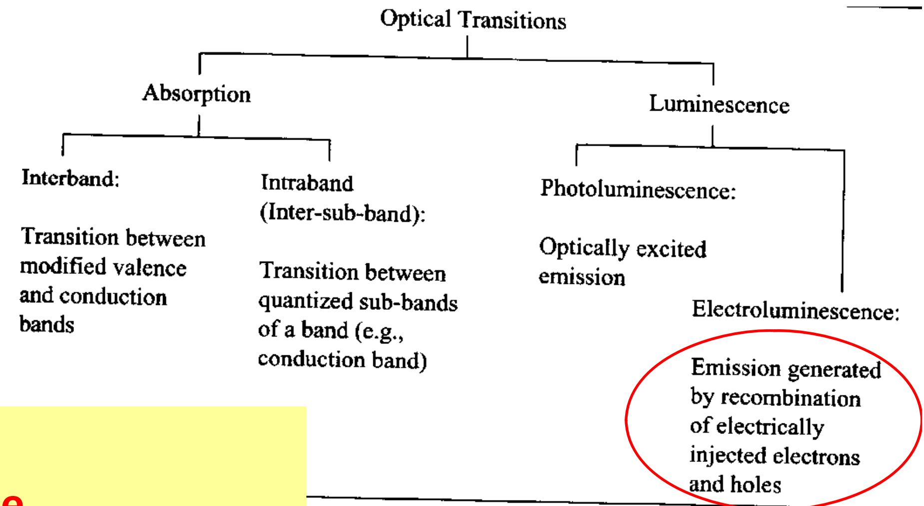

✓Interband transition energy is no longer E_{GAP}
✓Intraband (intersubband) transitions available
✓Increased transition "strength" (oscillator strength)

ECCITONI

Whenever **electron and hole wavefunctions overlap** each other, a quasi-bound system can be formed called **exciton**

Il calcolo dell'energia di legame degli eccitoni può essere effettuato in modo analogo a quello delle impurezze nei semiconduttori se le bande di valenza e di conduzione sono sferiche e non degeneri. Analogamente a quanto visto nel cap. 11, si ricava che i livelli idrogenoidi (riferiti alla cima della banda di valenza) hanno energie date da:

Hydrogen-like energy levels!

$$E_n = E_g - \frac{\mu e^4}{2\hbar^2 \varepsilon^2} \frac{1}{n^2}, \qquad (12.107)$$

ove n è il numero quantico principale, ε la costante dielettrica, e μ la massa ridotta del complesso elettrone-buca

$$\frac{1}{\mu} = \frac{1}{m_e^*} + \frac{1}{m_h^*} \cdot \qquad (12.108)$$

Nei semiconduttori abbiamo visto che $\varepsilon \simeq 10$ e $\mu \simeq 0.5 m_e$, per cui l'energia di legame degli eccitoni sarà dell'ordine di qualche decina di meV. A causa della grande costante dielettrica l'eccitone è dunque debolmente legato e la distanza media elettrone-buca è dell'ordine di decine di distanze reticolari. Un eccitone con queste caratteristiche è chiamato eccitone di Wannier-Mott, e ne discuteremo

Electron and hole system bound by Coulomb forces

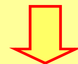

Exciton behaves like an hydrogen atom (but for some degeneracy removal, e.g., light and heavy hole states)

In (type I) quantum wells there is a high probability of exciton formation due to confinement of electrons and holes in the same layer

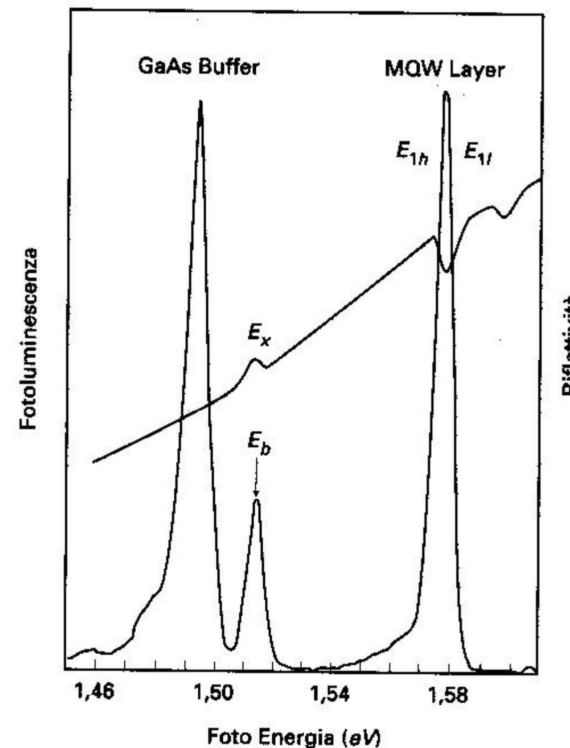

Figura 12.28
Fluorescenza eccitonica da un pozzo quantico (Q.W.) GaAs/$Ga_{1-x}Al_xAs$ e dal substrato GaAs a 12 K. E_b indica la posizione dell'eccitone nel substrato, E_{1h} ed E_{1l} gli eccitoni di buca pesante e di buca leggera nel Q.W. Per confronto è riportata anche la riflettività. Il picco di buca leggera compare soltanto ad alte temperature in fluorescenza, mentre è visibile in riflettività (Da Y. Chen, R. Cingolani, L.C. Andreani, F. Bassani e J. Massies, Il Nuovo Cimento D10, 847 (1988)).

A superlattice is formed by a periodic array of quantum structures (quantum wells, quantum wires, and quantum dots). An example of such a superlattice is a multiple quantum well, produced by growth of alternate layers of a wider bandgap (e.g., AlGaAs) and a narrower bandgap (GaAs) semiconductors in the growth (confinement) direction. This type of multiple quantum wells is shown in Figure 4.10a,b by a schematic of their spatial arrangement as well as by a periodic variation of their conduction and valence band edges.

When these quantum wells are widely separated so that the wavefunctions of the electrons and the holes remain confined within individual wells, they can be treated as a set of isolated quantum wells. In this case, the electrons (or the holes) can not tunnel from one well to another. The energies and wavefunctions of electrons (and holes) in each well remain unchanged even in the multiple quantum well arrangement. However, such noninteracting multiple quantum wells (or simply labeled multiple quantum wells) are often utilized to enhance an optical signal (absorption or emission) obtainable from a single well. An example is lasing, to be discussed in the next section, where the stimulated emission is amplified by traversing through multiple quantum wells, each well acting as an independent medium.

To understand the interaction among the quantum wells, one can use a perturbation theory approach similar to treating identical interacting particles with degenerate energy states. As an example, let us take two quantum wells separated by a large distance. At this large separation, each well has a set of quantized levels E_n labeled by quantum numbers $n = 1, 2, \ldots$ along the confinement direction (growth direction). As the two wells are brought close together so that the interaction between them becomes possible, the same energy states E_n of the two wells are no longer degenerate. Two new states E_n^+ and E_n^- result from the symmetric (positive) overlap and antisymmetric (negative) overlap of the wavefunctions of the well. The $E_n^+ = E_n + \Delta_n$ and $E_n^- = E_n - \Delta_n$ are split by twice the interaction parameter Δ_n for level n.

The magnitude of the splitting, $2\Delta_n$, is dependent on the level E_n. It is larger for higher energy levels because the higher the value of n (the higher the energy value E_n), the more the wavefunction extends in the energy barrier region allowing more interaction between the wells.

The case of two wells now can be generalized into the case of N wells. Their interactions lift the energy degeneracy to produce splitting into N levels, which are closely spaced to form a band, the so-called miniband. In an infinite multiple quantum well limit, the width of such a miniband is $4\Delta_n$, where Δ_n is the interaction between two neighboring wells for the level n. This result is shown in Figure 4.11 for the two levels E_1 and E_2 for the case of a superlattice consisting of alternate layers of GaAs (well) and $Al_{0.11}Ga_{0.89}As$ (barrier), each of width 9 nm. For this system, the miniband energies are $E_1 = 26.6$ meV and $E_2 = 87$ meV, with the respective bandwidth of $\Delta E_1 = 2.3$ meV and $\Delta E_2 = 20.2$ meV (Barnham and Vvedensky, 2001). As explained above, the higher-energy miniband (E_2) has a greater bandwidth (ΔE_2) than the lower energy miniband (ΔE_1).

MINIBANDE IN MQW

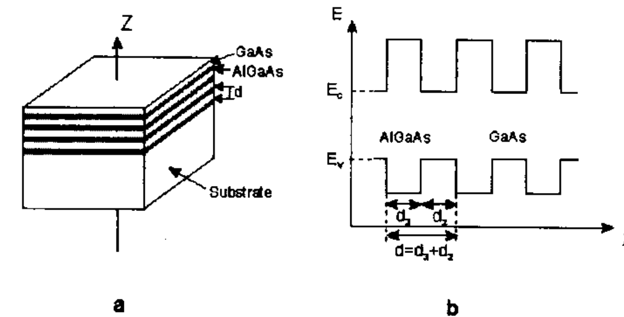

Figure 4.10. Schematics of the arrangement (a) and the energy bands (b) of multiple quantum wells.

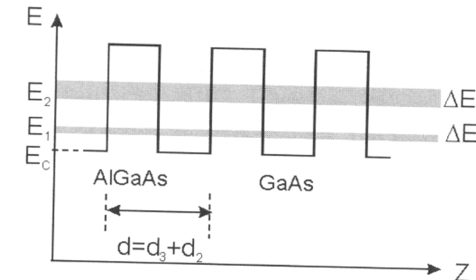

Figure 4.11. Schematics of formation of minibands in a superlattice consisting of alternate layers of GaAs (well) and AlGaAs (barrier).

- ✓ **"Minibands" formed due to interaction of different wells**
- ✓ **Consequences in QC lasers *(see later on!)***

LASER ETEROGIUNZIONE CONVENZIONALE

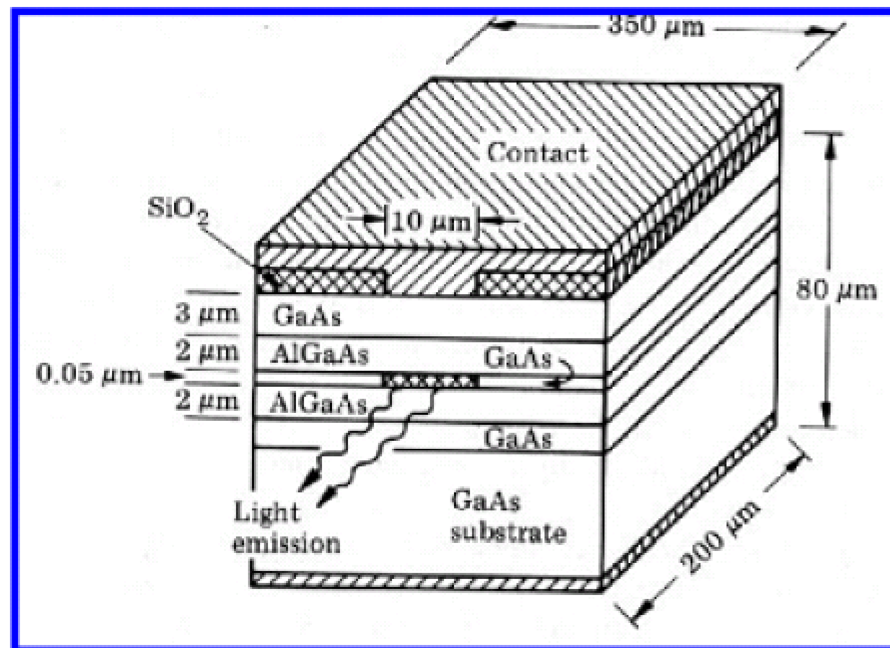

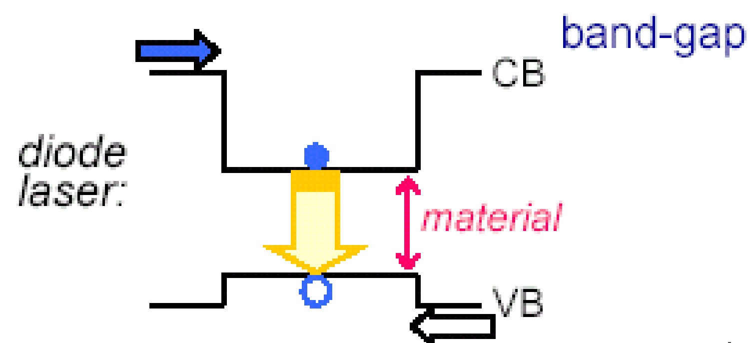

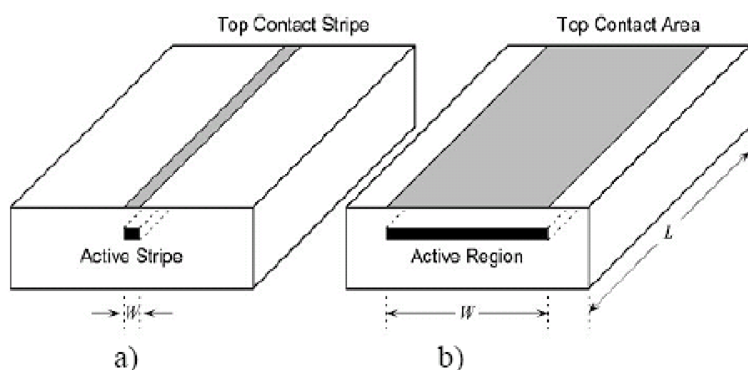

Figura 3.5.20 Esempi di *narrow and broad stripe geometries*

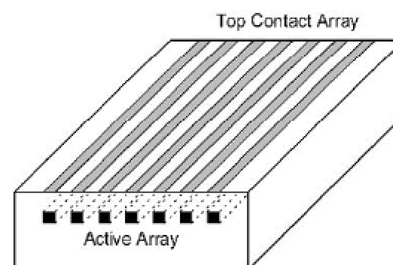

Figura 3.5.21
Laser ad *array*

Aumento di potenza attraverso aumendo volume mezzo attivo
Funzionamento generalmente impulsato (altrimenti problemi di dissipazione)
Potenze di picco fino a decine di W
Qualità ottica del fascio molto scarsa

EQUAZIONI DI BILANCIO DEL LASER A DIODO I

The laser diode rate equations model the electrical and optical performance of a laser diode. This system of ordinary differential equations relates the number or density of photons and charge carriers (electrons) in the device to the injection current and to device and material parameters such as carrier lifetime, photon lifetime, and the optical gain.

The rate equations may be solved by numerical integration to obtain a time-domain solution, or used to derive a set of steady state or small signal equations to help in further understanding the static and dynamic characteristics of semiconductor lasers.

The laser diode rate equations can be formulated with more or less complexity to model different aspects of laser diode behavior with varying accuracy.

Multimode rate equations [edit]

In the multimode formulation, the rate equations model a laser with multiple optical modes. This formulation requires one equation for the carrier density, and one equation for the photon density in each of the optical cavity modes:

$$\frac{dN}{dt} = \frac{I}{eV} - \frac{N}{\tau_n} - \sum_{\mu=1}^{\mu=M} G_\mu P_\mu$$

$$\frac{dP_\mu}{dt} = \Gamma_\mu (G_\mu - \frac{1}{\tau_p}) P_\mu + \beta_\mu \frac{N}{\tau_n}$$

where:

M is the number of modes modelled, μ is the mode number, and subscript μ has been added to G, Γ, and β to indicate these properties may vary for the different modes.

Spectral Shift [edit]

Dynamic wavelength shift in semiconductor lasers occurs as a result of the change in refractive index in the active region during intensity modulation. It is possible to evaluate the shift in wavelength by determining the refractive index change of the active region as a result of carrier injection. A complete analysis of spectral shift during direct modulation found that the refractive index of the active region varies proportionally to carrier density and hence the wavelength varies proportionally to injected current.

Experimentally, a good fit for the shift in wavelength is given by:

$$\delta\lambda = k \left(\sqrt{\frac{I_0}{I_{th}}} - 1 \right)$$

where I_0 is the injected current and I_{th} is the lasing threshold current.

EQUAZIONI DI BILANCIO DEL LASER A DIODO II

The modal gain [edit]

G_μ, the gain of the μth mode, can be modelled by a parabolic dependence of gain on wavelength as follows:

$$G_\mu = \frac{\alpha N[1 - (2\frac{\lambda(t) - \lambda_\mu}{\delta\lambda_g})^2] - \alpha N_0}{1 + \epsilon \sum_{\mu=1}^{\mu=M} P_\mu}$$

where: α is the gain coefficient and ε is the gain compression factor (see below). λ_μ is the wavelength of the μth mode, $\delta\lambda_g$ is the full width at half maximum (FWHM) of the gain curve, the centre of which is given by

$$\lambda(t) = \lambda_0 + \frac{k(N_{th} - N(t))}{N_{th}}$$

where λ_0 is the centre wavelength for $N = N_{th}$ and k is the spectral shift constant (see below). N_{th} is the carrier density at threshold and is given by

$$N_{th} = N_{tr} + \frac{1}{\alpha \tau_p \Gamma}$$

where N_{tr} is the carrier density at transparency.

β_μ is given by

$$\beta_\mu = \frac{\beta_0}{1 + (2(\lambda_s - \lambda_\mu)/\delta\lambda_s)^2}$$

where

β_0 is the spontaneous emission factor, λ_s is the centre wavelength for spontaneous emission and $\delta\lambda_s$ is the spontaneous emission FWHM. Finally, λ_μ is the wavelength of the μth mode and is given by

$$\lambda_\mu = \lambda_0 - \mu\delta\lambda + \frac{(n-1)\delta\lambda}{2}$$

where $\delta\lambda$ is the mode spacing.

Gain Compression [edit]

The gain term, G, cannot be independent of the high power densities found in semiconductor laser diodes. There are several phenomena which cause the gain to 'compress' which are dependent upon optical power. The two main phenomena are spatial hole burning and spectral hole burning.

Spatial hole burning occurs as a result of the standing wave nature of the optical modes. Increased lasing power results in decreased carrier diffusion efficiency which means that the stimulated recombination time becomes shorter relative to the carrier diffusion time. Carriers are therefore depleted faster at the crest of the wave causing a decrease in the modal gain.

Spectral hole burning is related to the gain profile broadening mechanisms such as short intraband scattering which is related to power density.

To account for gain compression due to the high power densities in semiconductor lasers, the gain equation is modified such that it becomes related to the inverse of the optical power. Hence, the following term in the denominator of the gain equation :

$$1 + \epsilon \sum_{\mu=1}^{\mu=M} P_\mu$$

PROPRIETÀ OTTICHE LASER INDEX GUIDED

Description

The SLD1135VS is a index-guided red laser diode for Laser pointer. The wavelength is 20nm shorter than SLD1122VS.

Features

- Small astigmatism (7μm typ.)
- Small package (ϕ5.6mm)
- Single longitudinal mode
- Low operating voltage (2.5V Max)
- Max operating temperature = 40°C (Case temperature)

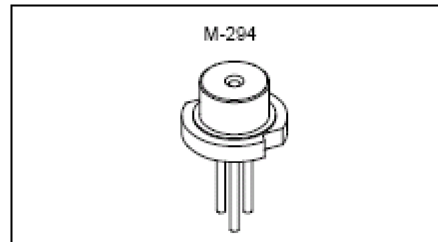

Asimmetria e astigmatismo fascio dovuti a forte asimmetria cavità (dimensioni diverse nelle varie direzioni)

Electrical and Optical Characteristics (Tc = 25°C) Tc: Case temperature

Item		Symbol	Conditions	Min.	Typ.	Max.	Unit
Threshold current		Ith			30	40	mA
Operating current		Iop	Po = 5mW		35	45	mA
Operating voltage		Vop	Po = 5mW		2.2	2.5	V
Wavelength		λp	Po = 5mW		650	660	nm
Radiation angle	Perpendicular	θ⊥	Po = 5mW	22	30	40	degree
	Parallel	θ//		5	7	12	degree
Positional accuracy	Position	ΔX, ΔY, ΔZ	Po = 5mW			±150	μm
	Angle	Δϕ//				±3	degree
		Δϕ⊥				±3	degree
Differential efficiency		ηD	Po = 5mW	0.3	0.6	0.9	mW/mA
Astigmatism		As	Po = 5mW		7	15	μm
Monitor current		Imon	Po = 5mW, V_R = 5V	0.05	0.1	0.25	mA

astigmatismo

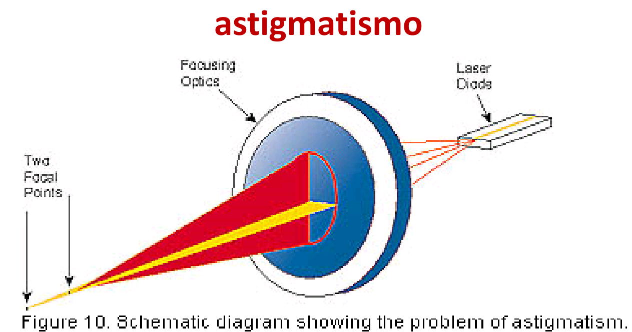

Figure 10. Schematic diagram showing the problem of astigmatism.

Fascio molto asimmetrico, divergente, astigmatico
Tipicamente bassa coerenza spaziale
Necessità di usare elevate aperture numeriche per buona focalizzazione o collimazione

PROPRIETÀ SPETTRALI LASER ETEROGIUNZIONE

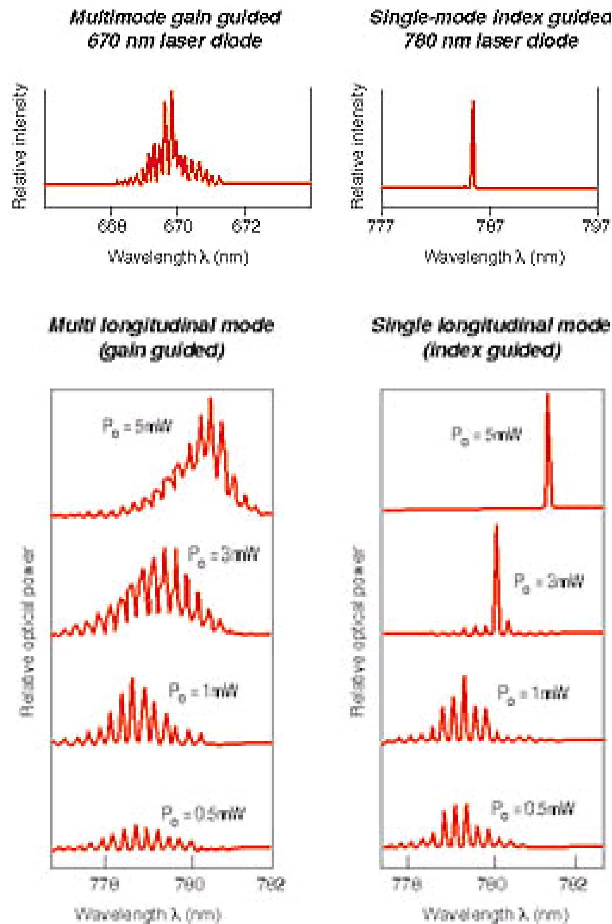

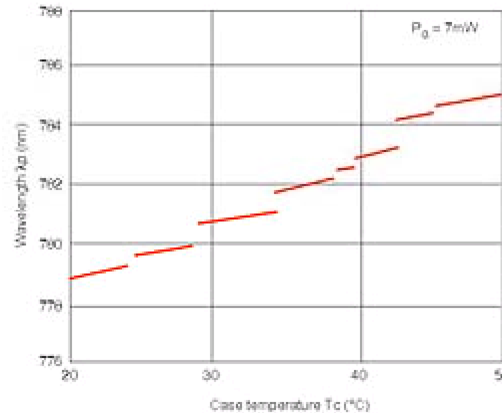

Figure 14. Mode hopping observed while temperature tuning a single-mode laser diode.

Salti di modo al variare di T → necessità di stabilizzare T (fino al mK)

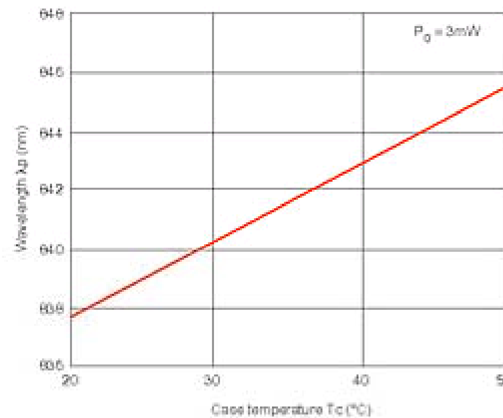

Figure 13. Effects of temperature on center wavelength.

Variazione lunghezza cavità (e indice di rifrazione) con T → Sintonizzabilità attraverso controllo di T (~0.2-0.4 nm/K)

Leggera dipendenza da corrente (~GHz/mA)

Normalmente competizione fra modi longitudinali

Nota: $\Delta\nu_C \sim 10^{11}$ Hz → modi spaziati di qualche Angstrom in lunghezza d'onda

CONTROLLO SPETTRO LASER ETEROGIUNZIONE

Accoppiamento ottico (feedback) con cavità esterna
→Sintonizzabilità (decina di nm)
→Aumento monocromaticità ($\Delta\nu_{L<1}$ < MHz)

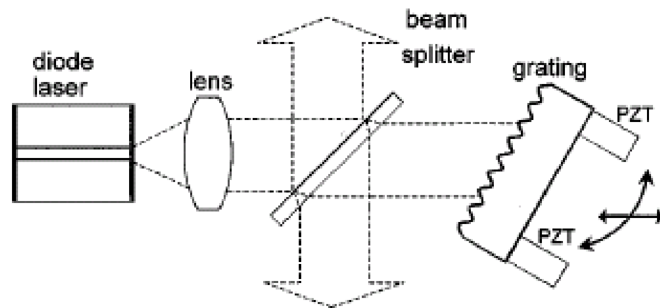

Consente stabilizzazione lunghezza d'onda tramite riferimento di frequenza e feedback sulla lunghezza della cavità esterna

Cavità risonanti integrate: DFB e DBR (ben sintonizzabili con temperatura)

DFB = Distributed FeedBack Laser - in which the grating is distributed along the entire active medium. The wavelength of the grating determines the wavelength emitted from the laser. This laser emits radiation in a very narrow line spectrum.

DBR = Distributed Bragg Reflector - in which the grating is outside the region of the active medium, in a place where no current flows (the passive part of the cavity).

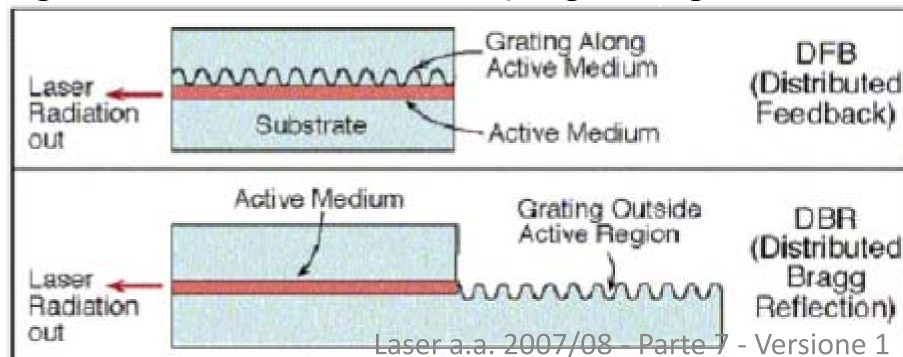

LASER A CAVITÀ VERTICALE (VCSEL)

Distributed Bragg Reflector structure (*1D photonic crystal)*

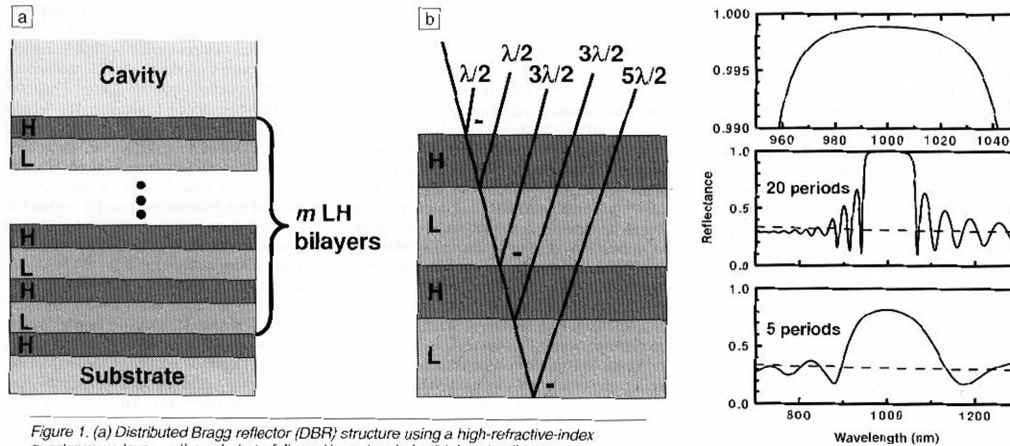

Figure 1. (a) Distributed Bragg reflector (DBR) structure using a high-refractive-index quarter-wave layer on the substrate followed by m low-index/high-index (LH) quarter-wave bilayers. (b) Relative phases at the DBR surface of light rays reflected from each interface within the DBR structure. The minus sign indicates the 180° phase shift that occurs upon reflection from a low- to high-index surface. A round-trip pass through each quarter-wave layer results in a half-wave phase shift. Every reflected ray returns to the DBR surface shifted by exactly 180° in phase. All reflected electric fields thus add constructively to give a high net reflectance for the DBR, even if individual interface reflectances are small.

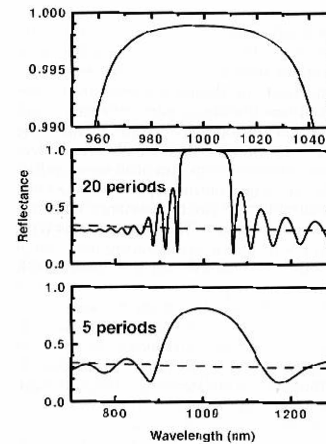

Figure 2. Reflectance spectrum in air of a 1000-nm GaAs/AlAs DBR for 20 periods and 5 periods (lower two plots). Dashed lines show the reflectance from a bare GaAs substrate. Top plot shows the high-reflectance region of the 20-period mirror near the design wavelength.

"Bragg mirrors" can be built by depositing alternate layers with different refractive index and highly controlled thickness

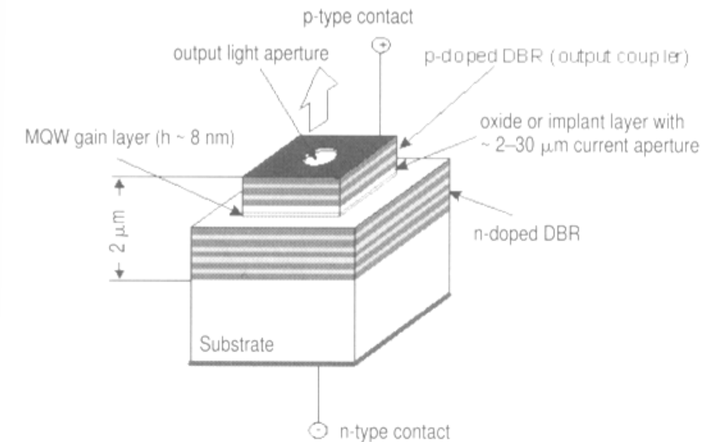

The laser cavity design discussed so far is that of an edge-emitting laser, also known as an in-plane laser, where the laser output emerges from the edge. However, many applications utilizing optical interconnection of systems require a high degree of parallel information throughput where there is a demand for surface emitting laser (SEL). In SEL the laser output is emitted vertically through the surface. Many schematics have been utilized to produce surface emitting lasers. A particularly popular geometry is that of a vertical cavity SEL, abbreviated as VCSEL. This geometry is shown in Figure 4.20. It utilizes an active medium such as multiple quantum wells sandwiched between two distributed Bragg reflectors (DBR), each comprising of a series of material layers of alternating high and low refractive indices. Thus for an InGaAs laser, the DBR typically consists of alternating layers of GaAs with refractive index ~3.5 and AlAs with refractive index 2.9, each layer being a quarter of a wavelength thick. These DBRs act as the two mirrors of a vertical cavity. Thus, both the active layer (InGaAs) and the DBR structures (GaAs, AlAs) can be produced in a continuous growth process.

An advantage offered by a VCSEL is that the lateral dimensions of the laser can be controlled, which offers the advantage that the laser dimensions can be tailored to match the fiber core for fiber coupling. An issue to deal with in VCSEL is the heating effect occurring in a complex multilayer structure, as the current is injected through a high series resistance of the DBRs.

Vertical Cavity Surface Emitting Laser

VCSEL advantages:

- Surface emission for integration in optoelectronics;
- "short" cavity: temp. stability, beam optical features, ...;
- Small overall size, low threshold, high efficiency

PROGRESSI NELLA FABBRICAZIONE

QC-laser crystal grown by
Molecular Beam Epitaxy (MBE)

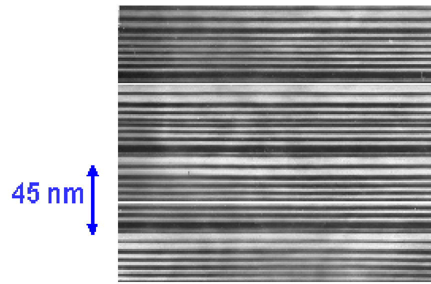

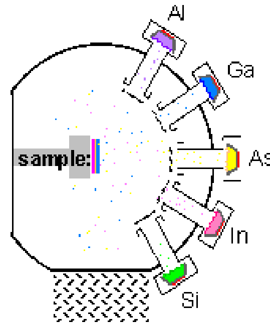

Cross-section of a few stages of QC-laser crystal ***crystal growth one atomic layer at a time***

- Many (~ 500), few-atoms thick layers of alloy materials (Al, Ga, As, In);
- atomic control of layer thickness, 1 nanometer (nm) = 4 atomic layers
- atomically flat layer interfaces

Progressi nella tecnica di fabbricazione MBE consentono negli ultimi anni di srealizzare dispositivi con migliori proprietà ottiche e di efficienza e di ottenere nuovi approcci

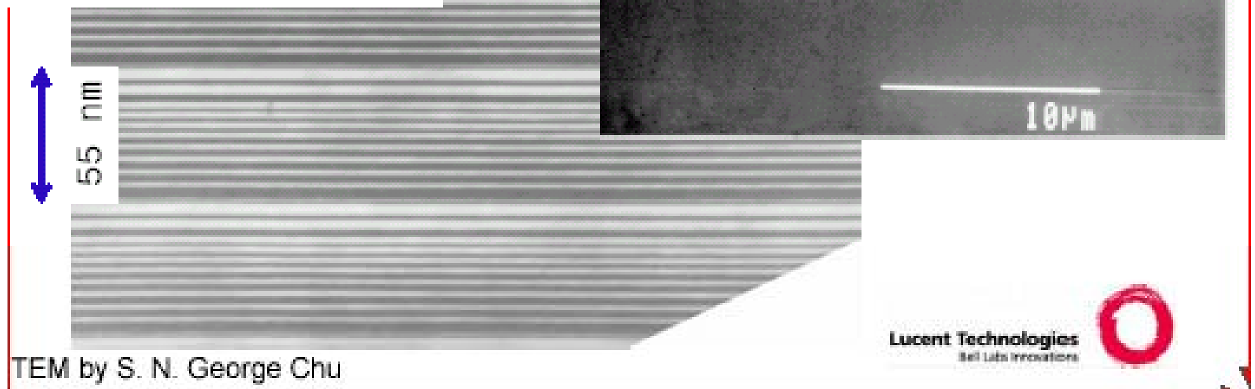

TEM by S. N. George Chu

LASER A CASCATA QUANTICA (QCL)

Completely new approach to lasing action with the goals:
-Mid-IR lasers with possibility to engineer wavelength (e.g., for trace analysis);
-Huge efficiency (low threshold, high power)

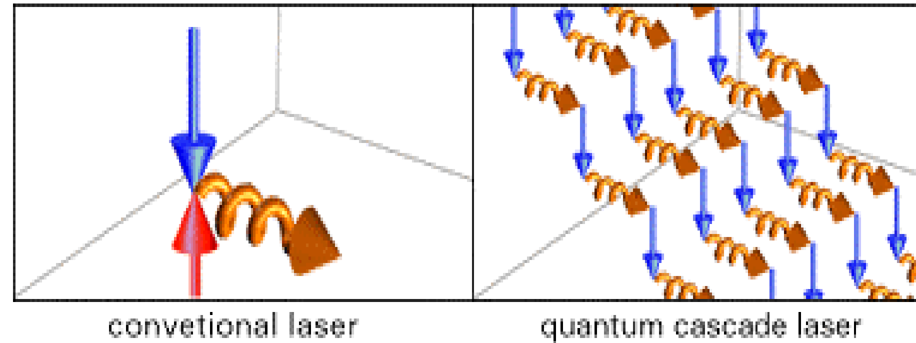

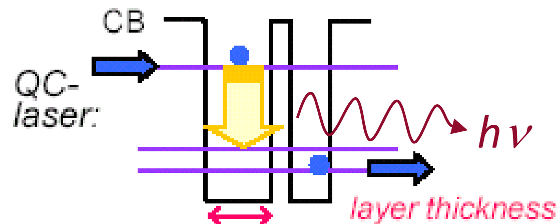

QC-laser:
Light is generated across designed energy ga
"materials by design":
band structure engineering and MBE

- In contrast to the lasers discussed above, which involve the recombination of an electron in the conduction band and a hole in the valence band, the QC lasers use only electrons in the conduction band. Hence they are also called unipolar lasers.
- Unlike the quantum-confined lasers discussed above, which involve an inter-band transition between the conduction band and the valence band, the QC lasers involve intraband (inter-sub-band) transition of electrons between the various sub-bands corresponding to different quantized levels of the conduction band. These sub-bands have been discussed in Section 4.1.
- In the conventional laser design, one electron at the most can emit one photon (quantum yield one). The QC lasers operate like a waterfall, where the electrons cascade down in a series of energy steps, emitting a photon at each step. Thus an electron can produce 25–75 photons.

QCL II

Figure 4.21 illustrates the schematics of the basic design principle of an earlier version of the QC lasers that produce optical output at 4.65 μm. These lasers are based on AlInAs/GaInAs. It consists of electron injectors comprised of a quantum well superlattice in which each quantized level along the confinement is spread into a miniband by the interaction between wells, which have ultrathin (1–3 nm) barrier layers. The active region is where the electron makes a transition from a higher sub-band to a lower sub-band, producing lasing action. The electrons are injected from left to right by the application of an electric field of 70 kV/cm as shown in the slope diagram. Under this field, electrons are injected from the ground state g of the mini-band of the injector to the upper level 3 of the active region. The thinnest well in the active region next to the injector facilitates electron tunneling from the injector into the upper level in the active region. The laser transition, represented by the wiggly arrow, occurs between levels 3 and 2, because there are more electron populations in level 3 than in level 2. The composition and the thickness of the wells in the active region are judiciously manipulated so that level 2 electron relaxes quickly to level 1.

The cascading process can continue along the direction of growth to produce more photons. In order to prevent accumulation of electrons in level 1, the exit barrier of the active region is, again, made thin, which allows rapid tunneling of electrons into a miniband of the adjacent injector. After relaxing into the ground state g of the injector, the electrons are re-injected into the next active region. Each successive active region is at a lower energy than the one before; thus the active regions act as steps in a staircase. Therefore, the active regions and the injectors are engineered to allow the electrons to move efficiently from the top of the staircase to the

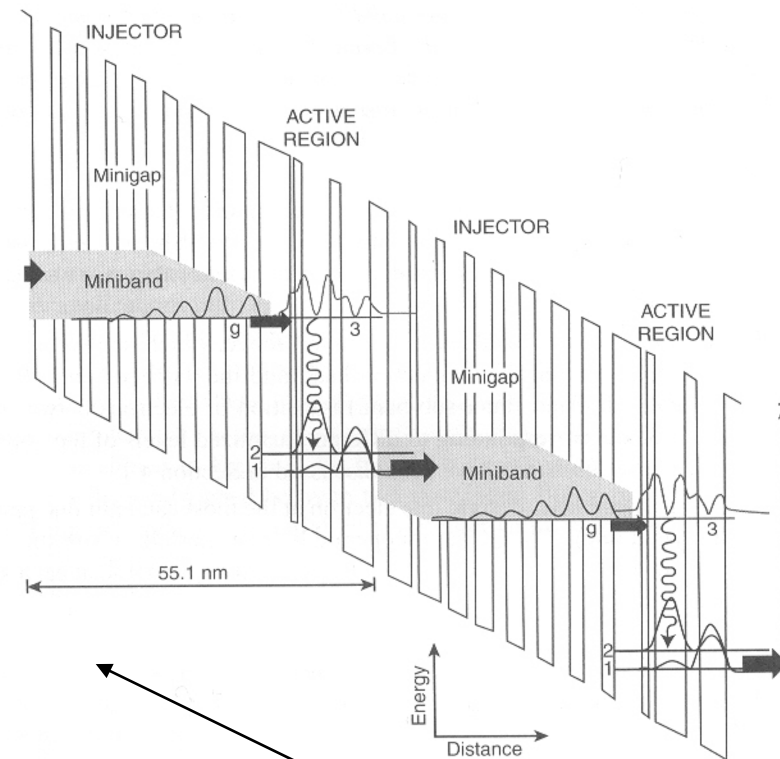

The slope is due to the electric field applied

Careful engineering and manufacturing of electron injector and active layers allow to achieve an efficient cascade behavior

QCL III

Quantum design of QC-laser

J. Faist, F. Capasso, C. Sirtori, D. L. Sivco, J. N. Baillargeon, A. L. Hutchinson, S. N. G. Chu, and A. Y. Cho, Appl. Phys. Lett. **68**, pp. 3680-3682 (1996).

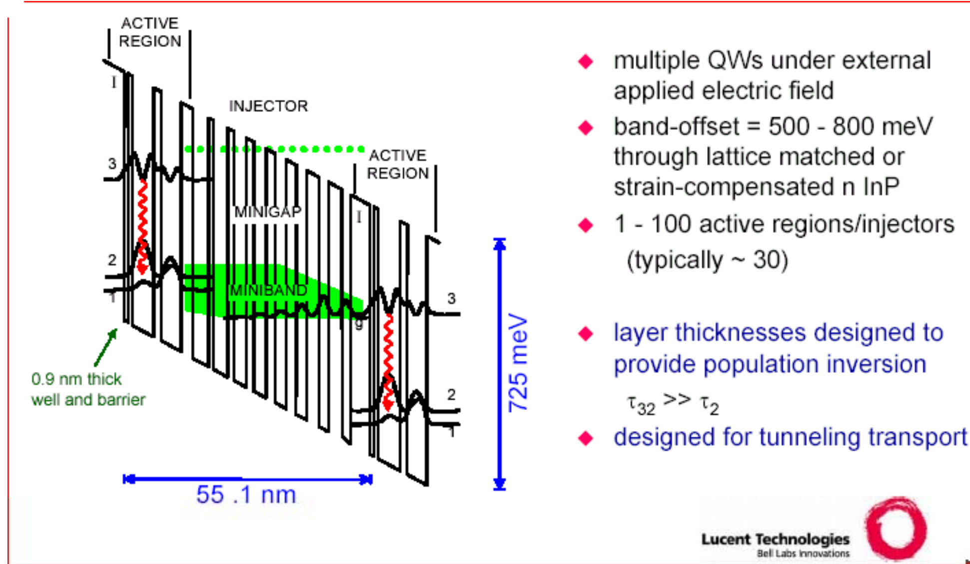

- multiple QWs under external applied electric field
- band-offset = 500 - 800 meV through lattice matched or strain-compensated n InP
- 1 - 100 active regions/injectors (typically ~ 30)
- layer thicknesses designed to provide population inversion

  $\tau_{32} >> \tau_2$
- designed for tunneling transport

Key characteristics of QC-lasers

- Wavelength ("color") determined by layer thickness rather than by material composition
- ➡ all mid-infrared spectrum covered by the same material
- Each electron creates N laser photons in traversing an N-stage cascaded structure (N = 20 - 75)
- ➡ intrinsically high power lasers
- High reliability: low failure rate, long lifetime and robust fabrication

Room temperature, pulsed, single-mode QC-DFB laser @ $\lambda \sim 4.65\ \mu m$

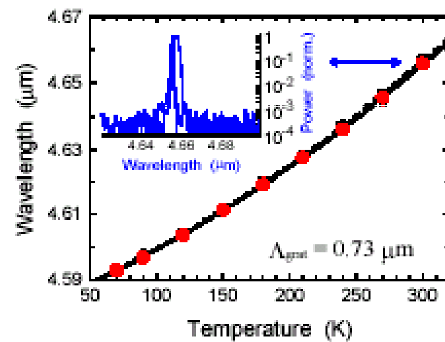

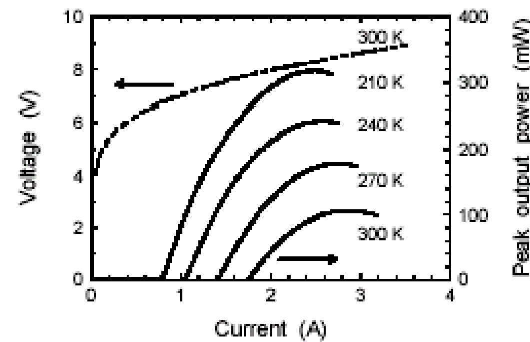

Wide wavelength-range of QC lasers

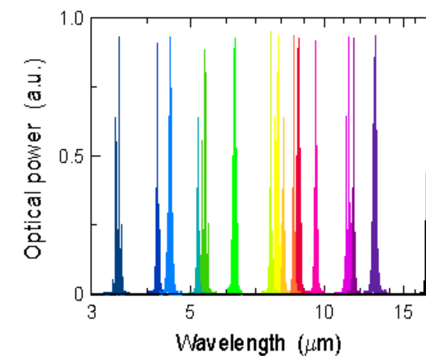

QC lasers cover entire mid-infrared wavelength range (3.4 - 17 µm) by tailoring layer thicknesses of the same material

CONCLUSIONI

Il laser a diodo (ad omogiunzione) sfrutta conoscenze già note negli anni '60

Lo sviluppo della tecnologia (MBE, in primis) ha permesso di ottimizzare architetture e fabbricazione negli anni '70-'80

Nuovi mercati consumer hanno spinto verso la diffusione dei laser a diodo

Oggi TLC, data storage, entertainment rendono i laser a diodo diffusi in modo universale e capillare

Esistono prospettive per nuovi ulteriori sviluppi

FONTI

O. Svelto and P. Hanna, Principles of Lasers (Plenum Press, 1998)
http://www.wikipedia.org
R. Pratesi, *Dispense di Fisica dei Laser*, Università di Firenze ed INO, (http://www.ino.it/home/pratesi/DispenseL&A.htm).
physics today, vari numeri
R. Waser (ed.), *Nanoelectronics and information technology* (Wiley-VCH, 2003)
F. Fuso, Fisica delle Nanotecnologie, trasparenze lezioni 2007/08, e referenze citate